AD-A092 382 ROCKWELL INTERNATIONAL THOUSAND OAKS CA SCIENCE CENTER F/G 11/3
LIFETIME PREDICTION OF ORGANIC COATING/METAL SYSTEM.(U)
AUG 80 F MANSFELD N00014-79-C-0437
UNCLASSIFIED SC5222.1AR NL

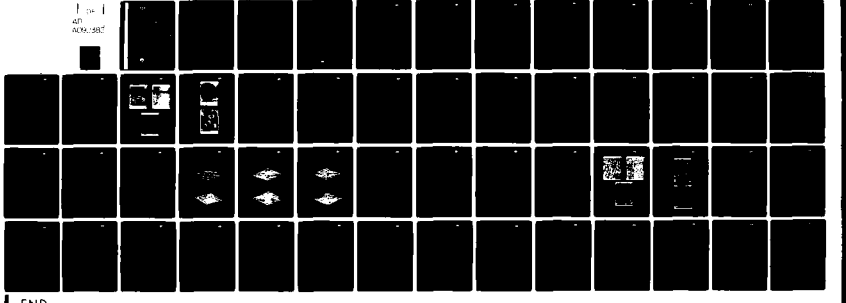

END
DATE FILMED
1-81
DTIC

LEVEL II

SC5222.1AR

Copy No. 18

LIFETIME PREDICTION OF ORGANIC COATING/METAL SYSTEM.

ANNUAL REPORT FOR THE PERIOD
1 July 1979 through 30 June 1980

GENERAL ORDER NO. 5222
CONTRACT NO. N00014-79-C-0437

Prepared for

Department of the Navy
Office of Naval Research
800 North Quincy Street
Arlington, VA 22217

Florian Mansfeld
Principal Investigator

AUG 80

12 54

Approved for public release; distribution unlimited

Rockwell International
Science Center

UNCLASSIFIED

SECURITY CLASSIFICATION OF THIS PAGE (When Data Entered)

REPORT DOCUMENTATION PAGE		READ INSTRUCTIONS BEFORE COMPLETING FORM
1. REPORT NUMBER	2. GOVT ACCESSION NO.	3. RECIPIENT'S CATALOG NUMBER
4. TITLE (and Subtitle) Lifetime of Organic Coatings/Metal Systems		5. TYPE OF REPORT & PERIOD COVERED Annual Report For Period 7/1/79 - 6/30/80
		6. PERFORMING ORG. REPORT NUMBER SC5222.1AR
7. AUTHOR(s) Florian Mansfeld		8. CONTRACT OR GRANT NUMBER(s) N00014-79-C-0437 NEW
9. PERFORMING ORGANIZATION NAME AND ADDRESS Rockwell International Science Center Thousand Oaks, CA 91360		10. PROGRAM ELEMENT, PROJECT, TASK AREA & WORK UNIT NUMBERS Project No. NR036-136(471)
11. CONTROLLING OFFICE NAME AND ADDRESS Office of Naval Research 800 North Quincy St., Arlington, VA 22217		12. REPORT DATE August 1980 13. NUMBER OF PAGES 47
14. MONITORING AGENCY NAME & ADDRESS(if different from Controlling Office) Dr. Philip A. Clarkin Director, Metallurgy & Ceramics Program, ONR 800 North Quincy Street, Arlington VA 2217		15. SECURITY CLASS. (of this report) UNCLASSIFIED 15a. DECLASSIFICATION/DOWNGRADING SCHEDULE

16. DISTRIBUTION STATEMENT (of this Report)

APPROVED FOR PUBLIC RELEASE: DISTRIBUTION UNLIMITED

17. DISTRIBUTION STATEMENT (of the abstract entered in Block 20, if different from Report)

18. SUPPLEMENTARY NOTES

19. KEY WORDS (Continue on reverse side if necessary and identify by block number)

Organic Coatings, Corrosivity, Surface Chemistry Analysis, AES, XPS, SEM
Surface Energetics Analysis, Surface Mapping.

20. ABSTRACT (Continue on reverse side if necessary and identify by block number)

The objective of this project is to develop a lifetime model which takes into account the corrosion susceptibility of metal substrates, the properties of organic coatings and the corrosivity of the environment.

The results obtained during the first year include the characterization of steel surfaces which had been subjected to different pretreatment methods using surface chemistry analysis (AES, XPS, SEM), surface energetics analysis, and surface mapping. The deposition kinetics and surface morphology of zinc—

(over)

DD FORM 1 JAN 73 1473 EDITION OF 1 NOV 65 IS OBSOLETE

UNCLASSIFIED

SECURITY CLASSIFICATION OF THIS PAGE (When Data Entered)

phosphate coatings on steel surfaces with different pretreatment have been studied with preliminary analysis using a.c. impedance techniques. These results provide a quantitative characterization of the substrate and provides input for a lifetime prediction model of polymer coated metal.

SC5222.1AR

LIFETIME PREDICTION OF ORGANIC COATING/METAL SYSTEM

Prepared for:
Department of the Navy
Office of Naval Research
800 North Quincy Street
Arlington, VA. 22217

Prepared by:
F. Mansfeld, J. Lumsden, S. Tsai, S. Jeanjaquet and M. Kendig
Rockwell International Science Center
Thousand Oaks, California 91360

Approved by

Ora E. Smith
Director
Structural Materials Integrity

Rockwell International
Science Center

TABLE OF CONTENTS

Page

LIST OF FIGURES.....iii
LIST OF TABLES..... iv
I. ABSTRACT..... 1
II. INTRODUCTION..... 2
III. RESULTS OBTAINED IN FIRST NINE MONTHS..... 3
1. Surface Cleaning Methods..... 3
2. Surface Analysis..... 5
3. Surface Energetics..... 10
4. Surface Mapping..... 21
5. Phosphate Conversion Coatings..... 26
a. Deposition Kinetics..... 26
b. Morphology..... 27
c. A.C. Impedance..... 32
IV. SUMMARY 44
V. REFERENCES..... 45
VI. APPENDIX: Surface Preparation Methods..... 46

LIST OF FIGURES

Figure		Page
1	SEM picture of steel after hot alkaline treatment	8
2	SEM picture of steel after degreasing	8
3	SEM picture of steel after the chemical smoothing process	8
4	SEM picture of steel after the anodic etch treatment	9
5	SEM picture of steel after mechanical polish and exposure to RH=80%, 1 ppm SO_2 for 19h	9
6	XPS spectrum (oxygen line) for steel pickled in inhibited HCl	11
7	XPS spectrum (oxygen line) for steel passivated in HNO_3	12
8	Changes of surface tension γ_{SV} as a function of time for 14 different surface pretreatments	14
9	Plot of dispersion α vs polar β components for different surface pretreatments	17
10	Ellipsometry data for mapping of sandblasted sample and sample which was degreased and cleaned with hot alkaline treatment	23
11	SPD maps for sandblasted and alkaline cleaned samples	24
12	PEE maps for sandblasted and alkaline cleaned samples	25
13	Potential-time curves for steel of four different surface pretreatments immersed in phosphating solution	28
14	Surface morphology of zinc phosphate conversion coating on steel for five different pretreatment procedures	30
15	Typical frequency dependence of $\|Z\|$ and θ for a phosphated steel: D+EP after 22 hours in 0.6 M KNO_3	34
16	Frequency dependence of $\|Z\|$ and θ for a phosphated steel (D+EP) in 0.06 M KNO_3 after 22 hours	37
17	Impedance analog for porous penetration model	38
18	Theoretical variation of θ spectrum with varied pore resistance	39
19	Variation of the frequency characteristics, ω_1 and ω_2, with time for D+EP specimens	40
20	Variation of the frequency characteristics, ω_1 and ω_2, with time for phosphated specimens	41
21	Theoretical variation of θ behavior under independent variation of the pore element	42

LIST OF TABLES

Table		Page
I.	Surface Preparation Methods for Steel	4
II.	Film Thickness, Film Composition, and Surface Morphologies Resulting from Various Treatments	6
III.	OH Content in Surface Films After Pretreatment (XPS Data)	10
IV.	Coating Weight, Metal Loss and Potential for Zinc-Phosphating of 1010 Steel	29
V.	Summary of the Results of Impedance Tests	36

I. ABSTRACT

The objective of this project is to develop a lifetime model which takes into account the corrosion susceptibility of metal substrates, the properties of organic coatings and the corrosivity of the environment.

The results obtained during the first year include the characterization of steel surfaces which had been subjected to different pretreatment methods using surface chemistry analysis (AES, XPS, SEM), surface energetics analysis, and surface mapping. The deposition kinetics and surface morphology of zinc phosphate coatings on steel surfaces with different pretreatment have been studied with preliminary analysis using a.c. impedance techniques. These results provide a quantitative characterization of the substrate and provides input for a lifetime prediction model of polymer coated metal.

II. INTRODUCTION

The objective of this program is to develop methodology for predicting the lifetime of organic coatings/metals systems in different aggressive environments. The approach is to use the Science Center capabilities in electrochemical corrosion research and in modern surface analysis techniques with inputs from efforts in the areas of polymer science and adhesion research. The information for the proposed modeling study will be obtained from the following five tasks which are interrelated:

I. Surface Pretreatment and Adhesion of Organic Coatings
II. Characterization of Paint Properties
III. Environmental Influences on Coatings Performance
IV. Techniques for Detection of Corrosion under Organic Coatings
V. Life Time Prediction Model

In this report the results of Task I are reported.

In studying the effects of various pretreatment and cleaning procedures for steel and Al alloys, it was considered very important to use methods which find wide practical application. The procedures defined in MIL-S-5002 and TT-C-490 were therefore chosen as a base line. In order to be able to get more detailed information about surface characteristics resulting from various pretreatment procedures, additional methods such as electropolishing, activation in acids, passivation by immersion or under applied potentials and a few other methods were used which can be considered to produce a wide spectrum of surfaces with different activity.

The surfaces are initially characterized by the scanning electron microscope (SEM), scanning Auger microscopy (SAM), surface energetics measurements and by surface mapping techniques. The next step is the application of phosphate conversion coatings, the morphology of which has been characterized by observation in the SEM. Determination of the electrochemical characteristics of phosphated surface by AC impedance techniques have been carried out to evaluate the effects of the various surface pretreatment procedures.

III. RESULTS OBTAINED IN FIRST YEAR

1. Surface Cleaning Methods

It is the intent of this study to correlate surface properties after pretreatment with adhesion of coatings and corrosion protection. For this reason, a number of surface pretreatment methods which are used in practice as well as some methods which are expected to result in surfaces with quite different chemical structures and activity are being studied. The cleaning methods for steel were selected from specifications such as US Federal Specification TT-C-490B and the British Code of Practice CP3012:1972. In addition, a number of other surface cleaning procedures were used such as pickling, passivation and electropolishing.

Table I lists sixteen procedures which were initially selected after a study of government specifications and various monographs on this subject.[1-4] Federal Specification TT-C-490B entitled "Cleaning Methods and Pretreatment of Ferrous Surfaces for Organic Coatings," covers six pretreatment processes for chemical conversion coatings without, however, specifying the exact solution composition or the steps in a pretreatment procedure. Details of the methods I-III, V, and VI in TT-C-490 (No. 1-5 in Table I) are contained in Appendix I. The British Code CP3012 has sections on preparation of steel surfaces prior to the application of surface coatings. Methods No. 6 to 9 are taken from this document; however, only the anodic etch and the chemical smoothing treatments were used more extensively.

For solvent cleaning, the samples were degreased by wiping with trichloroethylene followed by liquid/vapor degreasing for 15 min. Some samples were wet polished first with 600 SiC paper. Sandblasting was carried out with 10 μm Al_2O_3 powder.

The steel used throughout this study was 1010 steel (0.5 mm thick) in the as-received condition.

Table I

Surface Preparation Methods for Steel

No.	Treatment	Spec.	Solution	Time/Temperature	Remarks
1	Sandblasting	TT-C-490 Method I			
2	Degreasing	TT-C-490 Method II	Trichloroethylene	15 min	
3	Hot Alkaline	TT-C-490 Method III		5 min/100°C	
4	Alkaline derusting	TT-C-490 Method V		10 min/50°C	Type II
5	Phosphoric Acid	TT-C-490 Method VI		5 min/70°C	
6	Anodic Etch	CP3012 Method H.1	H_2SO_4	2 min/RT	0.1 A/cm^2
7	Chemical Smoothing	CP3012 Method L	$H_2C_2O_4$, H_2O_2 H_2SO_4	10 min/RT	
8	Acid Pickling	CP3012 Method F.6	HF/HNO_3	2 min/65°C	
9	Acid Dipping	CP3012 Method G.1	H_2SO_4	<2 min/70-85°C	
10	Pickling		42 v/o HCl + Inhibitor	5 min/RT	2-butyne-1,4-diol
11	Passivation I		Borate buffer	1 h/RT	+ 0.60 V vs SCE
12	Passivation II		1N H_2SO_4	1 h/RT	+ 1.00 V vs SCE
13	Passivation III		50 w/o HNO_3	30 min/RT	
14	Electropolish I		HNO_3/AC_2O	30 s/RT	
15	Electropolish II		$HClO_4$/BuOH/MeOH	1 min/-20°C	
16	Sulfuric dichromate		$H_2SO_4/Na_2Cr_2O_7/H_2O$	10 min/60°C	

2. Surface Analysis

The effects of the various surface pretreatments in Table I on surface morphology and the chemical composition of surface films were investigated using scanning electron microscopy (SEM) and surface analysis techniques such as scanning Auger microscopy (SAM) and XPS. The pretreatments were applied to both surfaces which were degreased only and to mechanically polished surfaces. The experiments with mechanically polished samples were carried out to evaluate whether the various pretreatment procedures would leave behind any residues on the sample surfaces, while the "degreased only" samples were tested to evaluate the effectiveness of the cleaning procedures. The cleaning procedures used include both those which are used as pretreatment procedures prior to the application of a coating and those which produce surfaces having known corrosion properties. The latter will provide baseline data for assessing the pretreatment procedures.

Table II gives film thickness, composition, and surface morphology resulting from the various treatments for both the "polished and degreased" and "degreased only" conditions.

In general, the surface conditions for both types of samples were the same following the same pretreatment. There were three exceptions: degreasing only failed to remove some calcium salts, which were removed, however, by additional mechanical polishing, and the acid dipping and the sulfuric and dichromate pretreatments, which left different amounts of copper on the surface depending on whether the surface was polished or not.

From Table II, on the basis of thickness, the films resulting from the various treatments can be divided into two groups: those of less than 50A thickness, and those thicker than 50A. In most cases the films having thicknesses of less than 50A resulted from passivation treatments or from treatments in which the surface was undergoing active dissolution. The films resulting from the latter treatments were formed by air oxidation after the samples were removed from solution. The films labeled as greater than 50A ranged from 75A to 250A in thickness.

Table II.

Film Thickness, Film Compositions, and Surface Morphologies Resulting from Various Treatments

Treatment	*Polished and Degreased*			*Degreased Only*		
	Thickness (Å)	Composition	Morphology	Thickness (Å)	Composition	Morphology
Sandblasting	>50	Oxide, Cl, S, C, Ca, Si, Al	Very Rough	>50	Oxide, Cl, S, C, Ca, Si, Al	Very Rough
Degreasing	<50	Oxide + Cl + C	Original	<50	Oxide + Cl + C, Ca	Original
Hot Alkaline	-	-	-	>50	Fe oxide + SiO_3	Original
Alkalin derusting	-	-	-	>50	Oxide, low S, low Cl	Original
Phosphoric Acid	-	-	-	<50	Oxide, high S, high P	Original
Anodic Etch	<50	Oxide, no S	Pits*	<50	Oxide, no S	GB etched, smoothed
Chemical Smoothing	-	-	-	<50	Oxide, no S	GB etched, smoothed
Acid Pickling	>50	Oxide + Cu + S	Smooth, inclusions not dissolved	>50	Oxide + Cu + S	Smooth, inclusions not dissolved
Acid Dipping	<50	Oxide, high S, Cu	Etched	>50	Oxide + high S	Etched
Pickling	<50	Oxide, high S, low Cl	Smooth	<50	Oxide, high S, low Cl	Smooth
Passivation I	<50	Oxide	Smooth	-	-	-
Passivation II	<50	Oxide + high S	Etched & Pits*	-	-	-
Passivation III	<50	Oxide, low S	Etched	>50	Oxide, low S	Etched
Electropolish I	>50	Oxide	Etched	>50	Oxide	GB etched
Electropolish II	<50	Oxide, high Cl + S	Etched	-	-	-
Sulfuric + Dichromate	<50	Oxide, high Cl + S	Smooth	>50	Oxide, high S, Cl, Cu	Etched
42% HCl	<50	Oxide, low Cl	GB Etched	-	-	-
Mechanical Polish	<50	Oxide, low S, low Cl	Smooth	-	-	-

GB = grain boundary

*Pits are apparently due to dissolution of sulfides.

All films were iron oxides or hydroxides with the exception of the film resulting from exposure to the hot alkaline cleaning solution. In this case, large amounts of silicate were incorporated in the film due to the presence of the inhibitor (sodium metasilicate). All samples exposed to sulfate solutions, with the exception of the anodic etch treatment, had films with high sulfur concentrations. This suggests that iron sulfate salts are present on the surface. Most films resulting from other treatments had low to moderate sulfur concentrations which likely resulted from the dissolution of sulfide inclusions in the steel. In some cases pits could be observed on the surface from which inclusions had been dissolved. Copper was found on the surfaces of samples which had been exposed to HNO_3 + HF (acid pickling) and hot H_2SO_4 (acid dipping). The copper was dissolved from the metal and then redeposited onto the surface. Its presence would have a deleterious corrosion effect on an uncoated surface. The most contaminated surface was produced by sandblasting with apparently impure material. High concentrations of salts, SiO_2 and Al_2O_3 were detected. Subsequent cleaning by sandblasting was performed with clean Al_2O_3. It is also of interest to note that after degreasing a 3-4 monolayer coverage of the trichloroethylene degreasing solution remained on the surface.

The morphology of the surface depends upon the treatment used. The hot alkaline treatment (Fig. 1) does not change the surface morphology when compared to the "degreased only" (Fig. 2) and leaves surface irregularities, inclusions, etc. Those treatments which had high anodic potentials etched the grain boundaries (Fig. 3). Passivation treatments in acidic solutions roughened the surface; whereas, the passivation treatment in borate buffer left the surface morphology unchanged.

Treatments which dissolve sulfide inclusions (Fig. 4) such as the anodic etch produce very corrosion resistant surfaces. The sulfide inclusions act as initiation sites for rusting. An example of this is shown in Fig. 5, which shows a mechanically polished steel surface after it has been exposed to an 80% relative humidity + 1 ppm SO_2 atmospheric condition for 19 hours. Disc-shaped rust spots can be observed on the surface. These spots were not present after exposure in the absence of SO_2. A scanning Auger analysis showed that a

Fig. 1 SEM picture of steel after hot alkaline treatment.

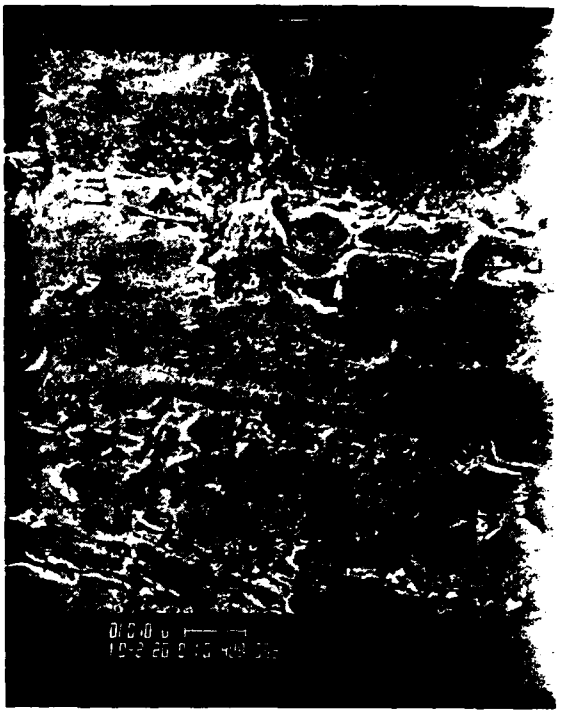

Fig. 2 SEM picture of steel after degreasing.

Fig. 3 SEM picture of steel after the chemical smoothing process.

Fig. 4 SEM picture of steel after the anodic etch treatment.

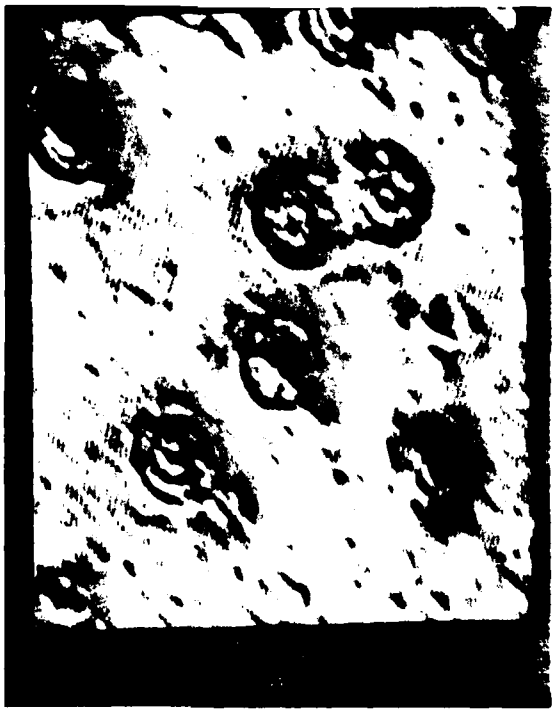

Fig. 5 SEM picture of steel after mechanical polish and exposure to RH=80%, 1 ppm SO_2 for 19h.

sulfide inclusion was located at the center of each disc. On the contrary, a surface which was pickled in inhibited 42 v/o HCl before exposure to the above conditions was unattacked (see also discussion of the mapping experiments below).

Figures 6 and 7 show the x-ray photoelectron spectra (XPS) of oxygen for surfaces pickled in inhibited HCl and passivated in concentrated HNO_3, respectively. A shoulder at higher binding energies is observed for the pickled specimen which arises from the presence of OH in the film. This shoulder is not present for the sample passivated in HNO_3. As suggested by these two spectra large variations were observed in the OH concentrations for films formed in the different pretreatment procedures. A summary for treatments which gave high, low to moderate and no hydroxide concentrations in the surface films is given in Table III.

Table III

OH Content in Surface Films After Pretreatment (XPS-Data)
(1018 Steel, all samples were polished, 1 μm finish)

No OH	Low to moderate	High
Conc. HNO_3	Anodic Etch	Electropolish II
Electropolish I	Chemical Smoothing	Degreased
	$H_2SO_4 + Na_2Cr_2O_7$	Inhibited HCl

3. Surface Energetics

As discussed by Kaelble,[5] surface energetics analysis provides an important new tool in both materials selection and surface treatment. This technique has therefore been used to characterize steel surfaces after various pretreatment procedures from Table I. The wettability of such surfaces has been measured quantitatively and the nominal values for the solid-vapor surface tension γ_{SV} of such samples have been calculated. The experimental methods and analysis employed in this study have been described in detail by Kaelble and Dynes[6] who studied surface energetics of Al2024-T3. Liquid-solid contact

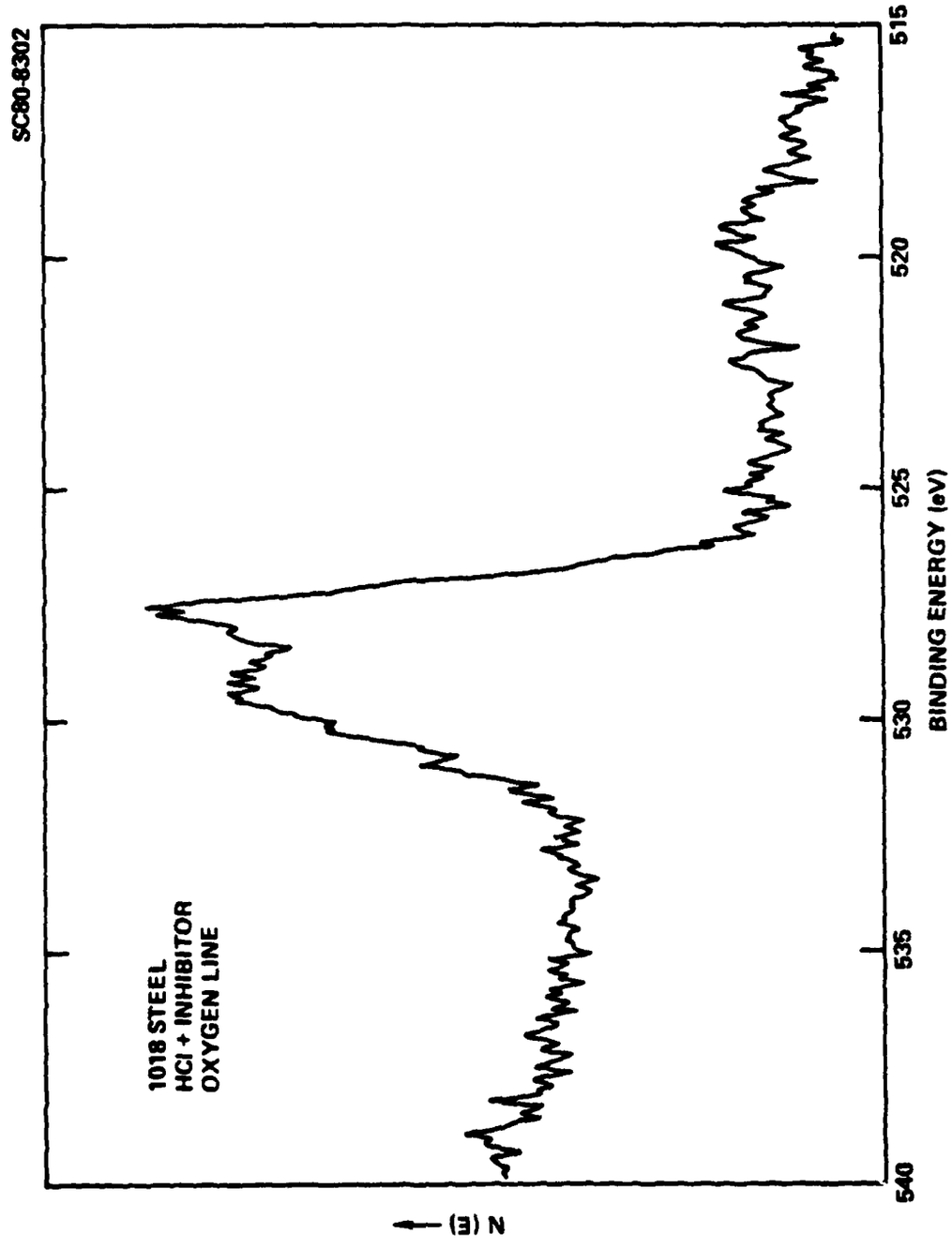

Fig. 6 XPS spectrum (oxygen line) for steel pickled in inhibited HCl.

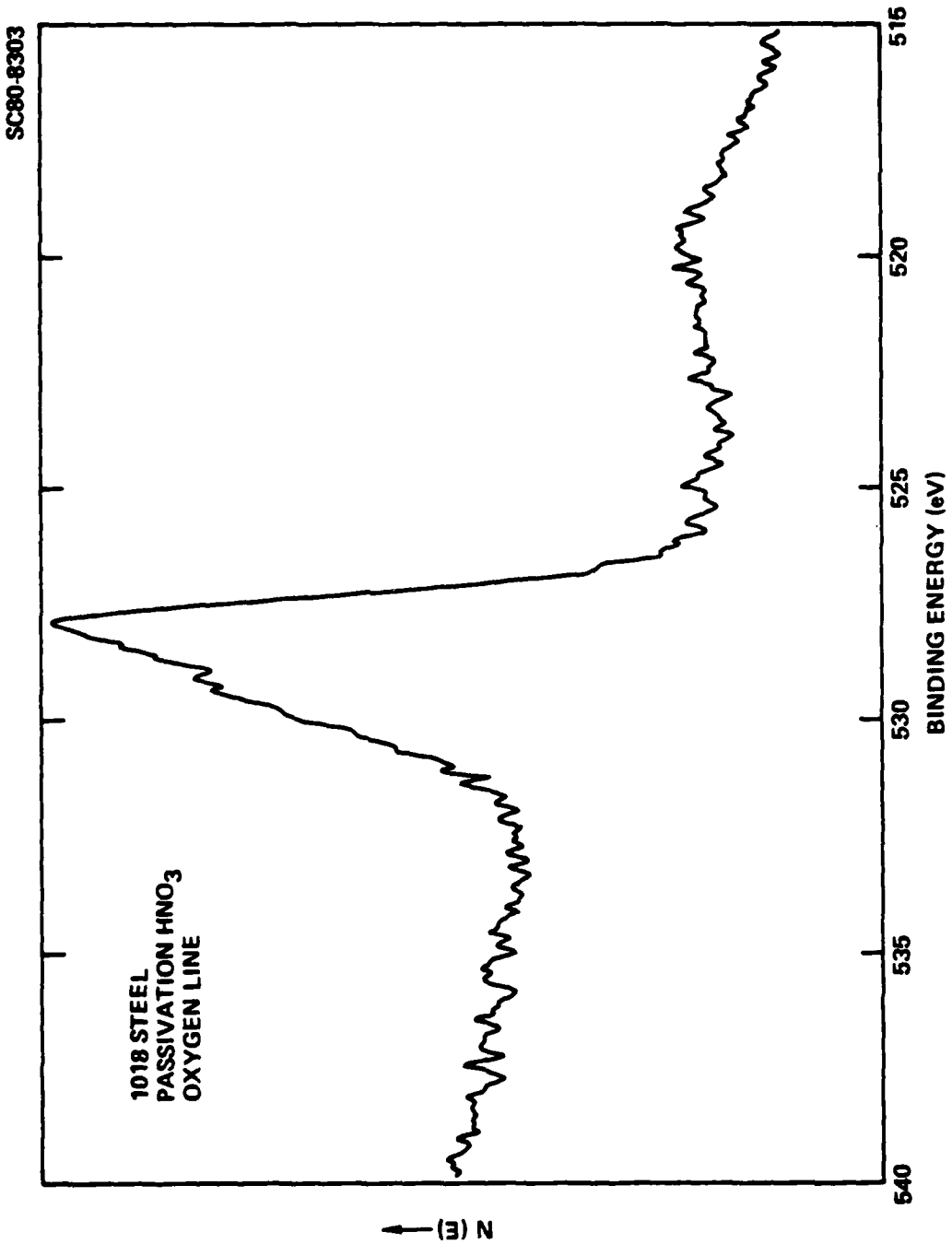

Fig. 7 XPS spectrum (oxygen line) for steel passivated in HNO_3.

angles are measured with calibrated liquids of known surface tension γ_{LV} and ratio of polar-dispersion character. The surface tension properties of the test liquids in this study are those used by Kaelble.[5] Contact angles were measured with a NRL goniometer (Rame-Hart) using the sessile drop method where the drop size is small (< 3 µl) to avoid gravitational flattening.

The dispersion (nonpolar) γ_{SV}^{d} and polar γ_{SV}^{p} components of $\gamma_{SV} = \gamma_{SV}^{d} + \gamma_{SV}^{p}$ have been calculated from the measured values of γ_{SV} as a function of time in order to detect changes in surface characteristics while the freshly prepared surfaces age in contact with the environment (laboratory air at RH = 30-45%).

Figure 8 a-c shows the changes of γ_{SV} with time for 14 different surface pretreatment. Most tests were terminated after 24h, however, some tests were conducted up to 160h. The magnitude of γ_{SV} and its time-dependence characterize the activity of different surfaces. The H_3PO_4, hot alkaline and H_2SO_4 + $Na_2Cr_2O_7$ treatments give the highest values of γ_{SV} without any significant changes with time. The passivation treatments in HNO_3, 1N H_2SO_4 and borate buffer initially produce higher γ_{SV} values; however, these surfaces are not stable (Fig. 8b). A polished sample which was pickled in inhibited HCl initially has higher γ_{SV} values than a sample which was degreased but not polished before pickling; however, after 24h the surface energetics of the two samples are almost identical. Exposure to humid air and SO_2 after pickling lower the surface tension (Fig. 8c).

More detailed information concerning the relative polar character of the surface result from plots which represent the surface characteristics as $\alpha = \sqrt{\gamma_{SV}^{d}}$ and $\beta = \sqrt{\gamma_{SV}^{p}}$. Highly polar surface exhibit low α and high β values. A plot of α vs β shows how the surface properties differ for different surface treatment and how aging affects these properties. The results for 15 different surface treatments of steel are plotted in Fig. 9a-d. In general, all data fall within the band shown in Fig. 9 which extends from polar characteristics at short times after treatment to more dispersive characteristics after longer times.

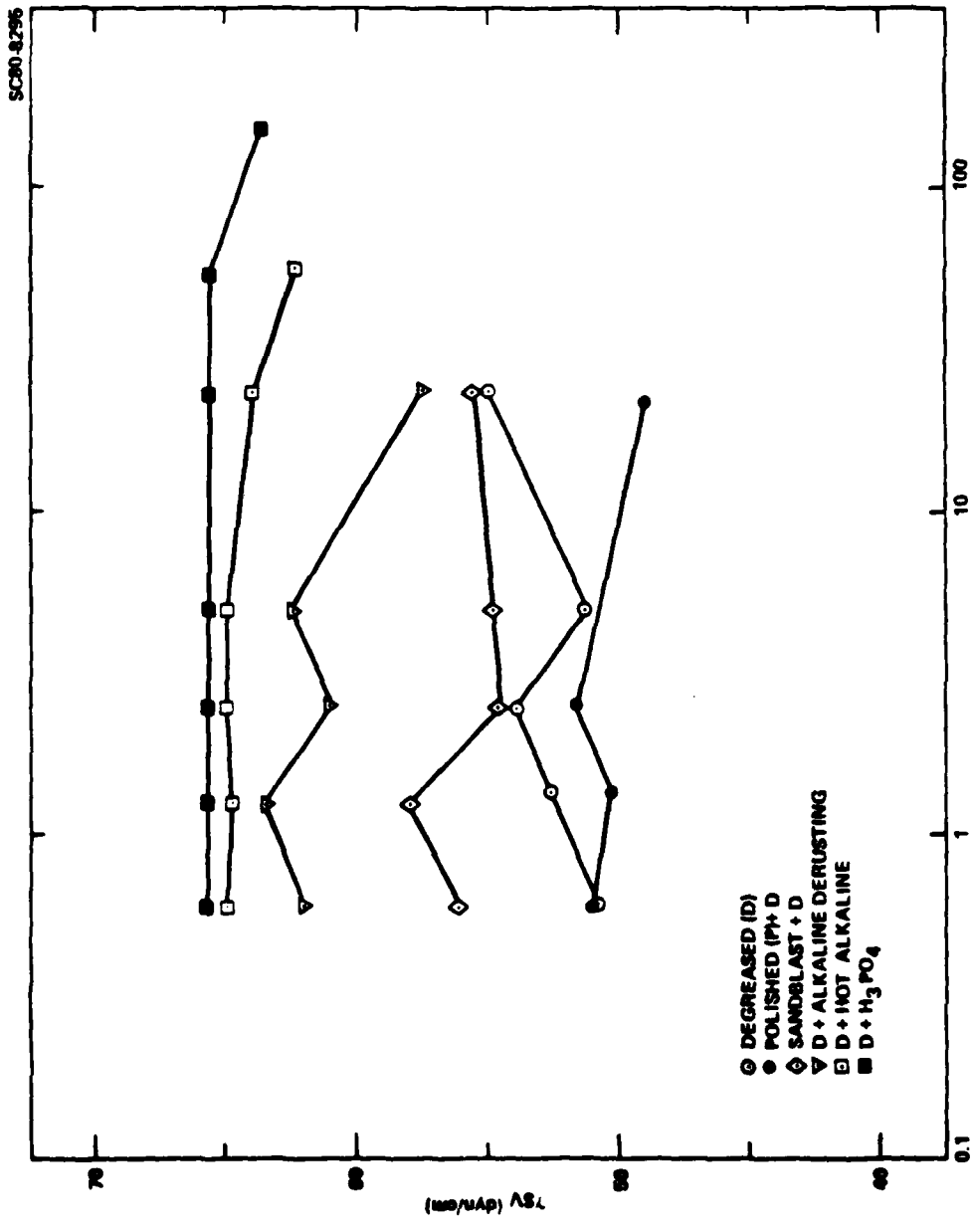

Fig. 8 Changes of surface tension γ_{SV} as a function of time for 14 different surface pretreatments.

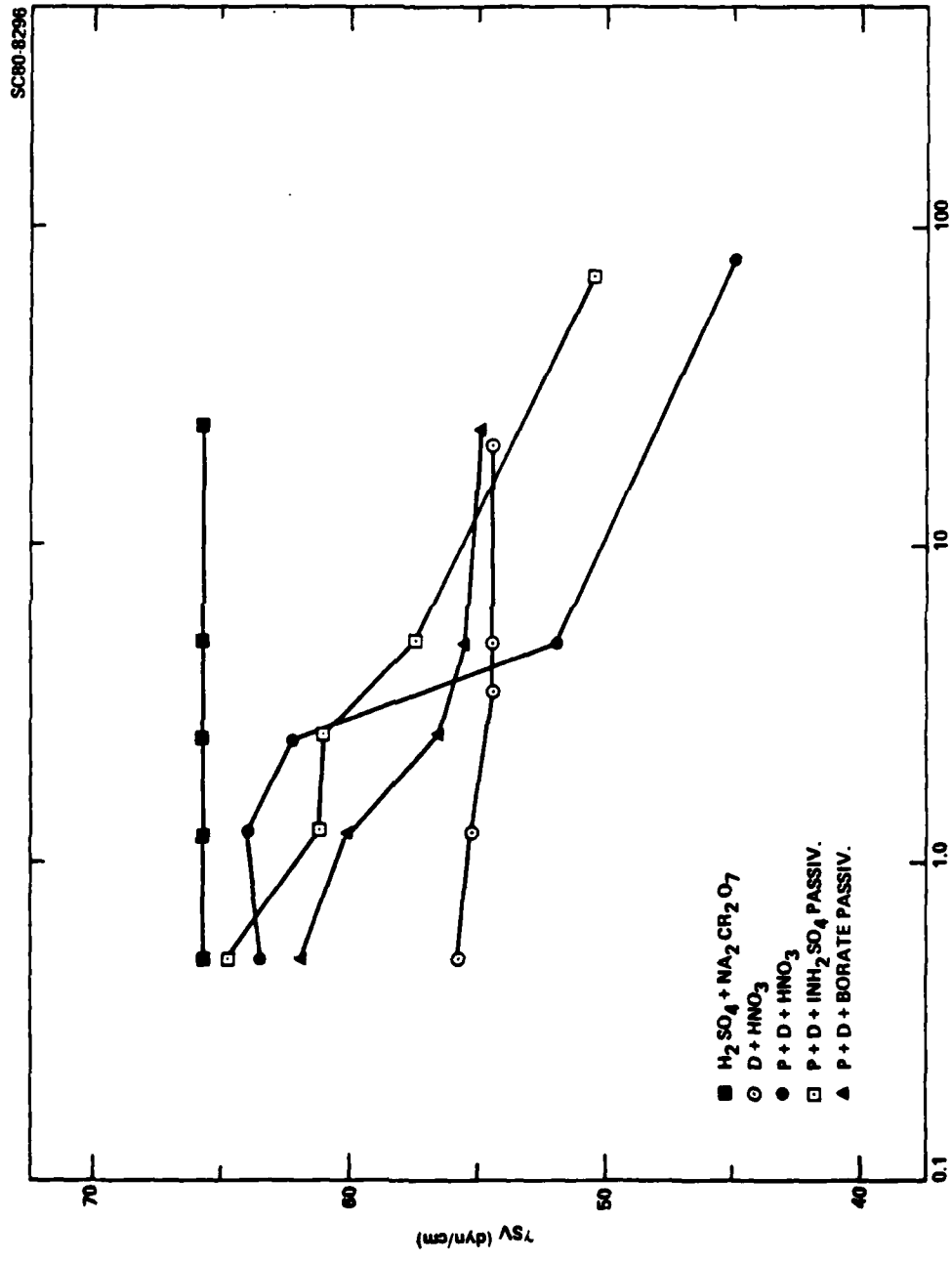
SC80-8296
$H_2SO_4 + NA_2CR_2O_7$
D + HNO_3
P + D + HNO_3
P + D + INH_2SO_4 PASSIV.
P + D + BORATE PASSIV.
TIME (H)
0.1
1.0
10
100
70
60
50
40
γSV (dyn/cm)

(b)

Fig. 8 (cont'd).

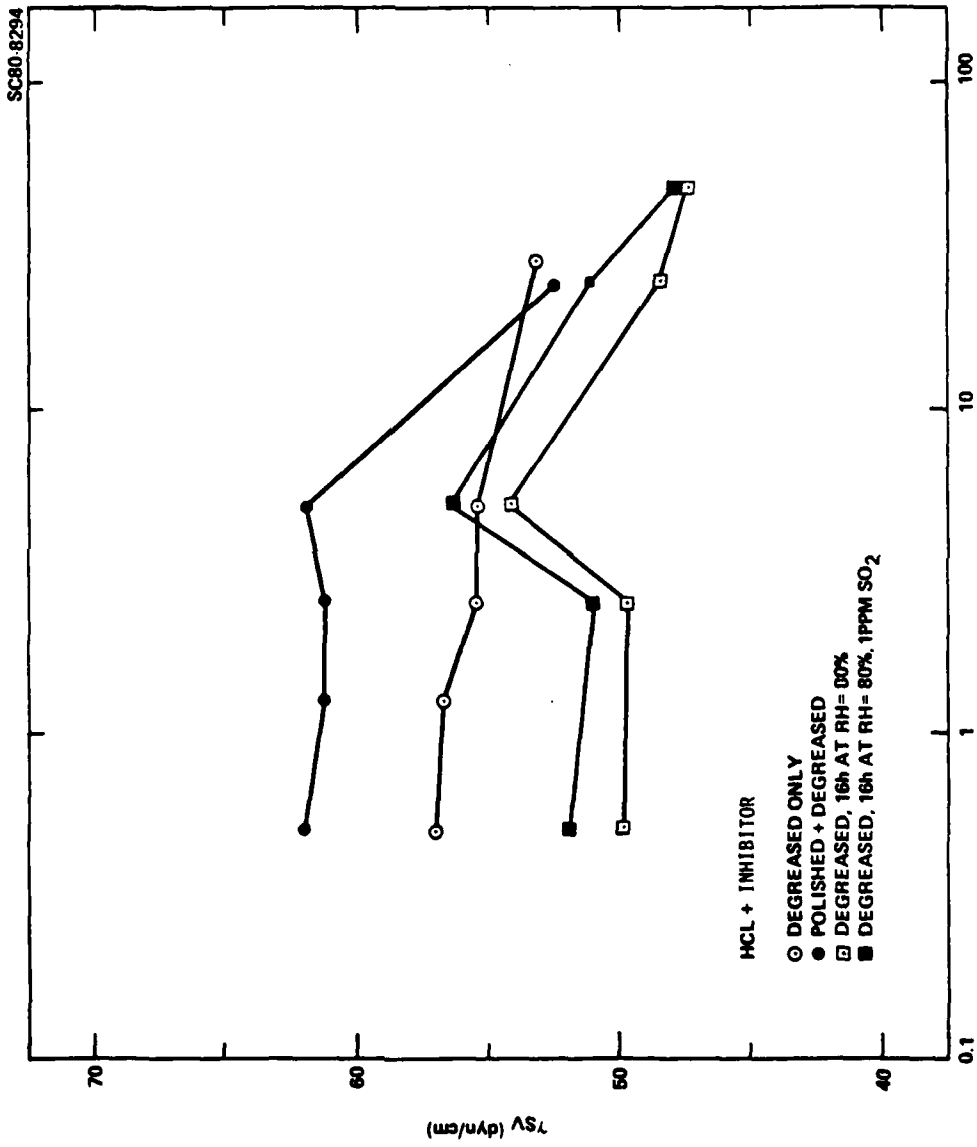
SC80-8294
HCL + INHIBITOR
⊙ DEGREASED ONLY
● POLISHED + DEGREASED
⊡ DEGREASED, 16h AT RH= 00%
■ DEGREASED, 16h AT RH= 80%, 1PPM SO_2
TIME (H)
γ_{SV} (dyn/cm)
70
60
50
40
0.1
1
10
100

(c)

Fig. 8 (cont'd).

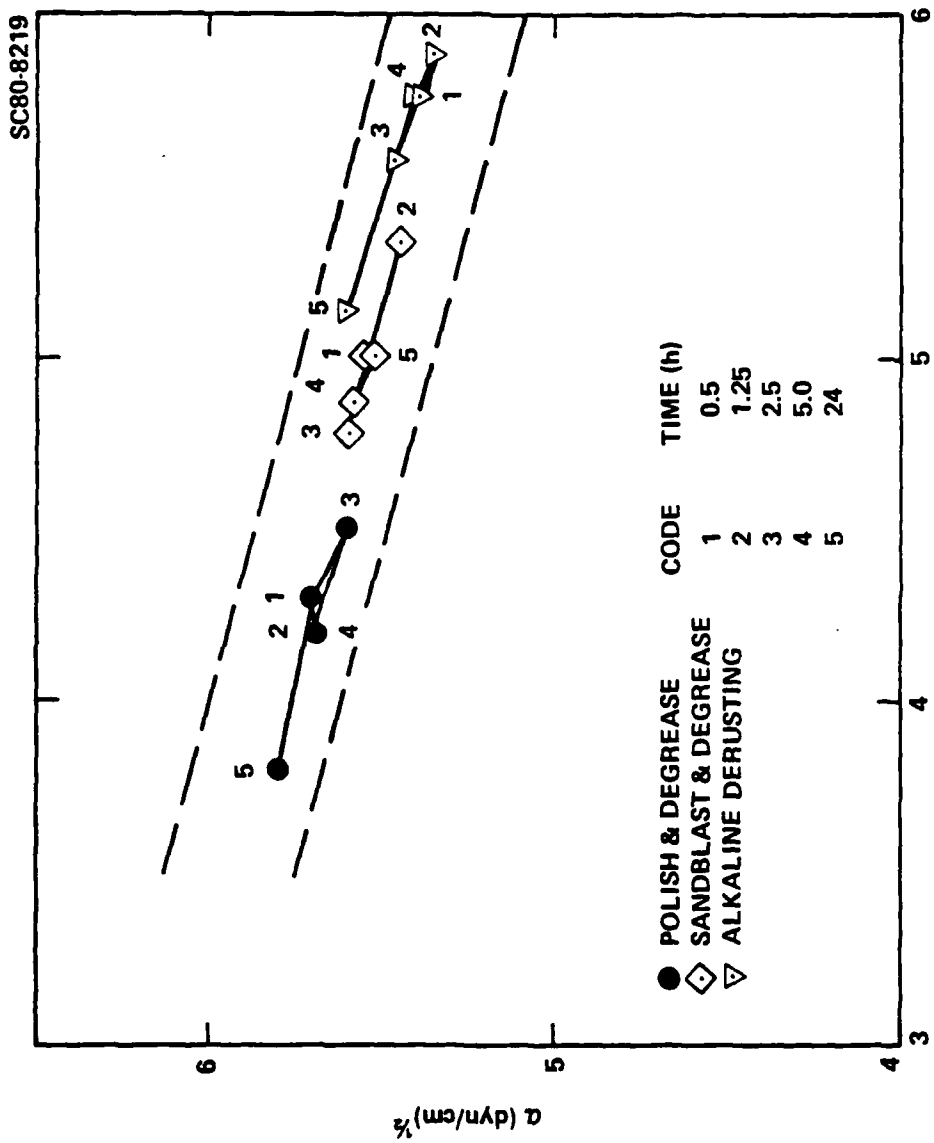

Fig. 9 Plot of dispersion α vs polar β components for different surface pretreatments.

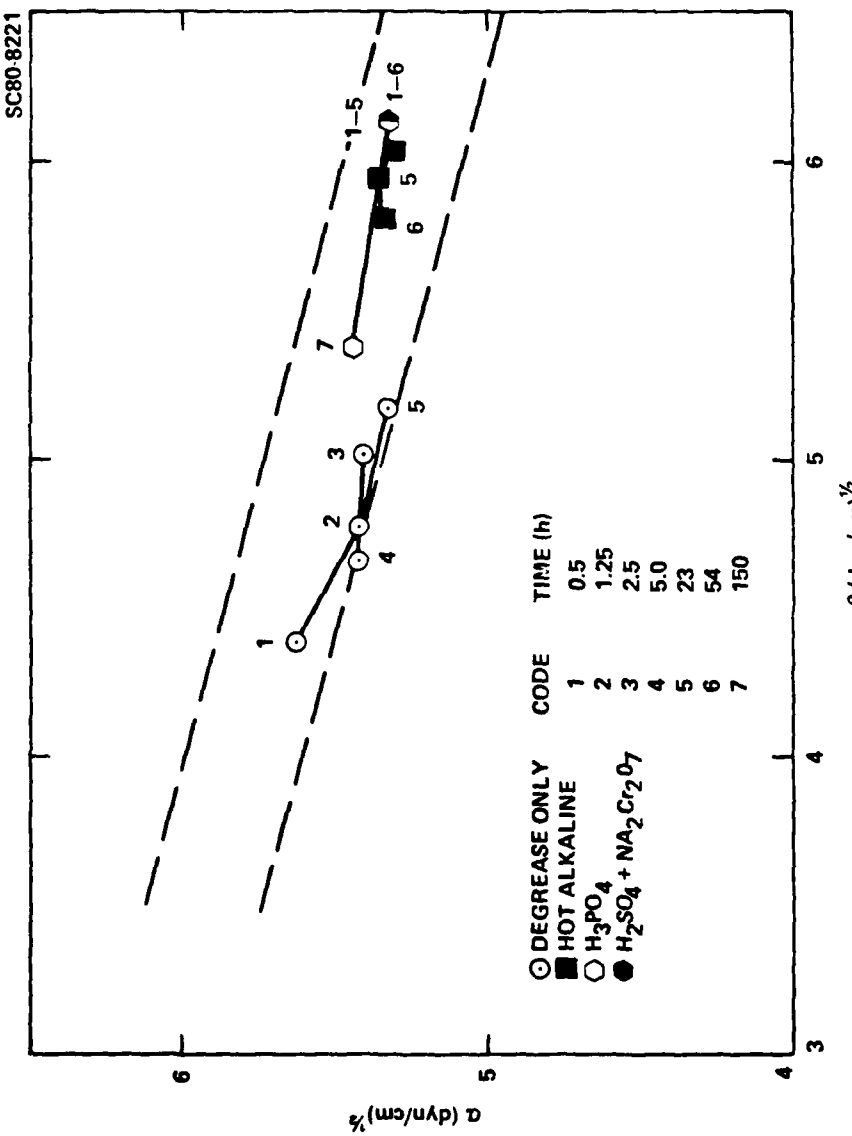
SC80-8221
α (dyn/cm)½
β (dyn/cm)½
DEGREASE ONLY
HOT ALKALINE
H3PO4
H2SO4 + NA2Cr2O7
CODE
TIME (h)
1 0.5
2 1.25
3 2.5
4 5.0
5 23
6 54
7 150
1–5
1–6

(b)

Fig. 9 (cont'd).

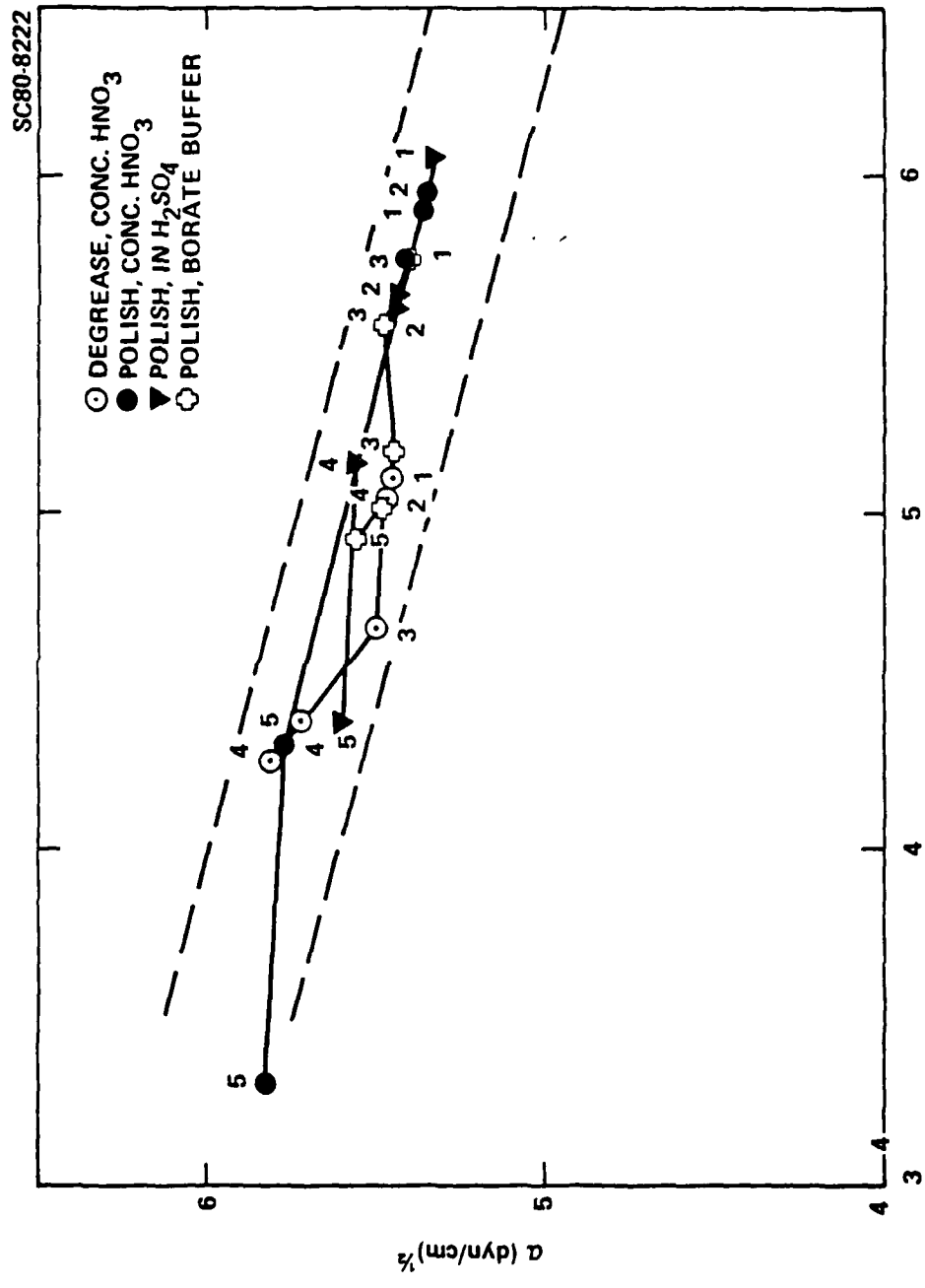
SC80-8222
DEGREASE, CONC. HNO_3
POLISH, CONC. HNO_3
POLISH, IN H_2SO_4
POLISH, BORATE BUFFER
α (dyn/cm)½
β (dyn/cm)½

(c)

Fig. 9 (cont'd).

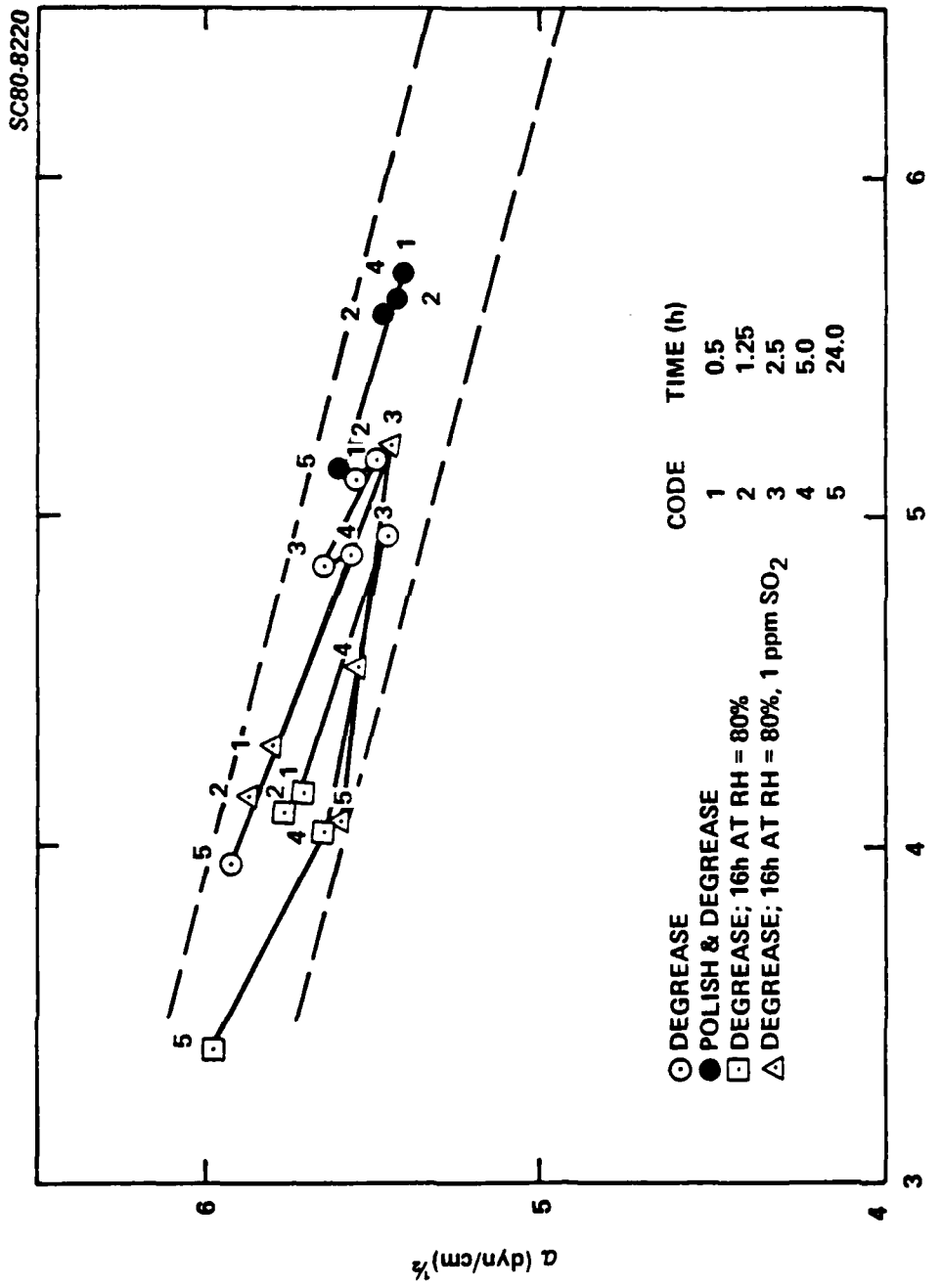
SC80-8220
α (dyn/cm)½
β (dyn/cm)½
CODE TIME (h)
1 0.5
2 1.25
3 2.5
4 5.0
5 24.0
⊙ DEGREASE
● POLISH & DEGREASE
⊡ DEGREASE; 16h AT RH = 80%
△ DEGREASE; 16h AT RH = 80%, 1 ppm SO2

(d)

Fig. 9 (cont'd).

Figure 9a shows a pronounced difference in surface properties of steel which was polished and degreased and steel which was sandblasted or treated by alkaline derusting. The latter two samples have a much more polar character which results from the outer surface hydroxyl ions or hydrated oxides. After 24h these surfaces are still much more polar than the surface which was polished and degreased only. A surface which was degreased but not polished changed to more polar character with time (Fig. 9b). Hot alkaline cleaning, the phosphoric acid and the $H_2SO_4/Na_2Cr_2O_7$ treatments produced surfaces which initially were completely wettable with highly polar character (Fig. 9b). Only very small changes occur with aging time for these treatments, after 150h the α and β values have changed somewhat for the H_3PO_4 treated surface (see also Fig. 9a).

Three different passivation treatments are compared in Fig. 9c. A surface which had been polished before passivation in HNO_3 initially was much more polar than a corresponding sample which had only been degreased before passivation. However, after 5h the surface properties were about equal. The point labelled "5" for the polished sample was taken after 78h. Passivation of polished samples in 1N H_2SO_4 and in borate buffer produces surfaces which are similar to those passivated in HNO_3. However, the changes to less polar characteristics are less pronounced than for this sample. The data point labelled "5" for passivation in 1N H_2SO_4 was taken after 70h (see also Fig. 9b).

The data for samples treated in inhibited HCl are shown in Fig. 9d. A sample which was polished and degreased before pickling was much more polar and more stable than a sample which had not been polished prior to pickling. Exposure of the unpolished, pickled sample to RH = 80% for 16h with or without 1 ppm SO_2 produced surfaces with a highly non-polar character which became more polar in the first 5h and then changed again to the initial properties.

4. Surface Mapping

When surfaces are prepared for coating, they are usually assumed to be spacially uniform and little attention is given to spacial heterogeneity. However, due to inclusions,surface history, contamination, etc., surfaces are likely to have some heterogeneity with respect to surface properties. Since the

coating adhesion under stress and corrosion is directly related to flaws at the coating-substrate interface, heterogeneity becomes of great significance. To discover surface heterogeneity we have developed an automated scanning facility that will map the surface of samples that have been prepared for coating in various ways. The surface properties that are mapped include optical properties (e.g. oxide or contamination thickness by ellipsometry), dielectric properties (surface potential difference (SPD) that is sensitive to the outer dipole layer) and electron emission and attenuation properties (by photoelectron emission (PEE)). A detailed description of the methods used in the measurements and their interpretation is given by Smith.[7]

Surface Mapping for Different Pretreatments

The mapping facility scans the samples and produces a map of the signal from each instrument (ellipsometry, SPD, PEE). A computer prints out the maximum and minimum values along with the average and standard deviation. Examples of ellipsometer maps for two surface treatments of steel are given in Fig. 10. Each map covers approximately 4 cm x 4 cm with a grid of 1 mm x 1 mm. The scattered light reveals the roughness of the sandblasted sample. The hot alkaline sample is much smoother and differs in the value of the phase shift (DELTA) which is related to the oxide film thickness. The film thickness of the hot alkaline cleaned sample is estimated ~ 10A and the sandblasted sample ~ 80A. Figure 11 compares SPD maps for these two surface treatments. The average SPD of the hot alkaline treated surface is -0.18 volts as compared to +0.11 volts for the sandblasted surface. Auger spectroscopy has shown that silicate contamination is at the outer surface of the hot alkaline cleaned samples (Table II). It is postulated that the $Si^{-O}Si$ structure exposes the electronegative oxygen which causes SPD to be negative. The sandblasted samples, on the other hand, are heavily contaminated with organics which usually expose hydrocarbons at the outer surface and oxygen bonds to the substrate, leaving the dipole orientation with the positive end outward. This accounts for the positive SPD for the sandblasted samples.

Figure 12 compares PEE maps for the same two surface treatments. The average PEE for the hot alkaline surface is 0.035 nA as compared to 0.044 nA for

NULL ELLIPS 4 APR 80

DEGREASED, SANDBLAST, DEGREASED - PREPARED 10:45, 4 APR 80
MAPPED 11:00, 4 APR 80
MAX = DELTA OF 79.0 DEG, MIN = DELTA OF 78.0 DEG
MIN =.3200E 03 UNITS
MAX =.4100E 03 UNITS
AVERAGE =.3670E 03 UNITS
STD DEVIATION =.1464E 02 UNITS

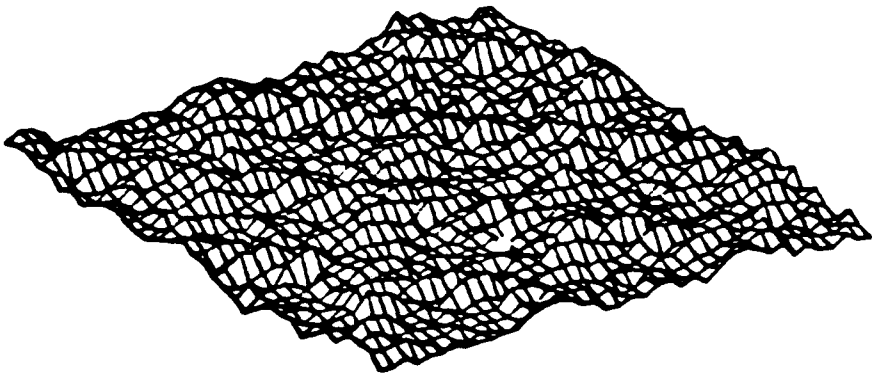

NULL ELLIPS 2 APR 80

HOT ALKALINE III - PREPARED 8:46, 2 APR 80
MAPPED 9:45, 2 APR 80
MAX = DELTA OF 96.6 DEG, MIN = DELTA OF 89.5 DEG
MIN =.0000E 00 UNITS
MAX =.7400E 03 UNITS
AVERAGE =.4998E 02 UNITS
STD DEVIATION =.4259E 02 UNITS

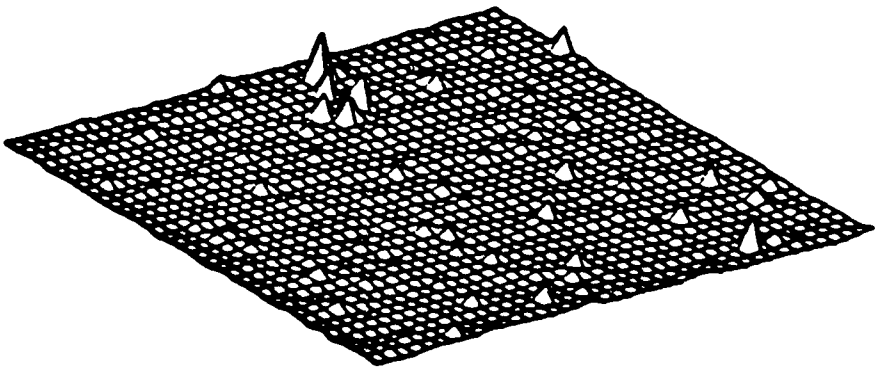

Fig. 10 Ellipsometry data for mapping of sandblasted sample and sample which was degreased and cleaned with hot alkaline treatment.

SPD 4 APR 80

DEGREASED: SANDBLAST, DEGREASED - PREPARED 10:45, 4 APR 80
MAPPED 11:25, 4 APR 80

MIN =.9589E-01 VOLTS
MAX =.1264E 00 VOLTS
AVERAGE =.1122E 00 VOLTS
STD DEVIATION =.5546E-02 VOLTS

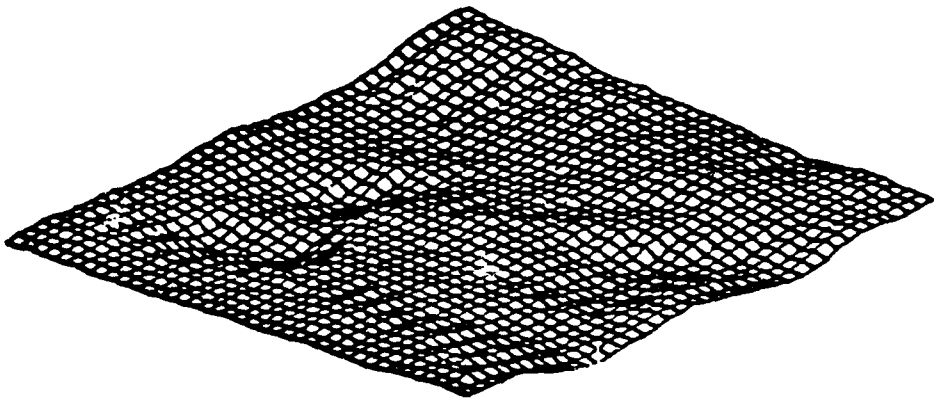

SPD 2 APR 80

HOT ALKALINE III - PREPARED 8:46, 2 APR 80
MAPPED 10:22, 2 APR 80

MIN =-.1253E 00 VOLTS
MAX =-.2234E 00 VOLTS
AVERAGE =-.1822E 00 VOLTS
STD DEVIATION =.1623E-01 VOLTS

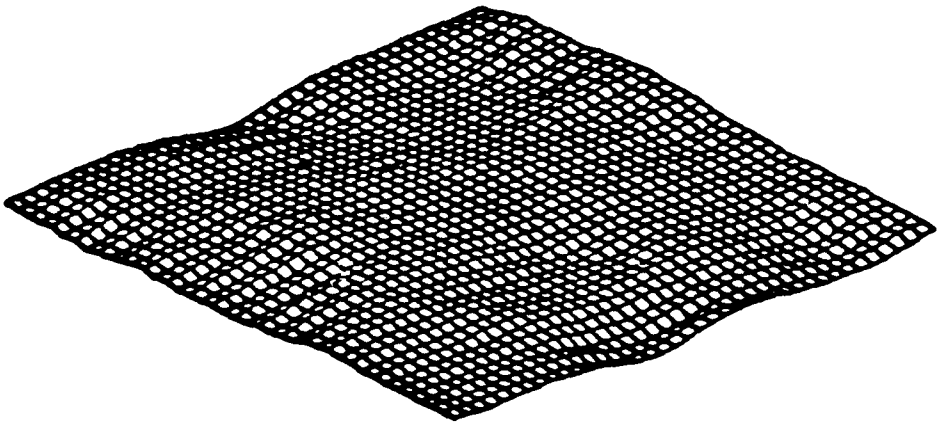

Fig. 11 SPD maps for sandblasted and alkaline cleaned samples.

PEE 4 APR 80

DEGREASED, SANDBLAST, DEGREASED - PREPARED 10:45, 4 APR 80
MAPPED 12:12, 4 APR 80

MIN =.3621E-01 NANO AMP
MAX =.6270E-01 NANO AMP
AVERAGE =.4498E-01 NANO AMP
STD DEVIATION =.1731E-01 NANO AMP

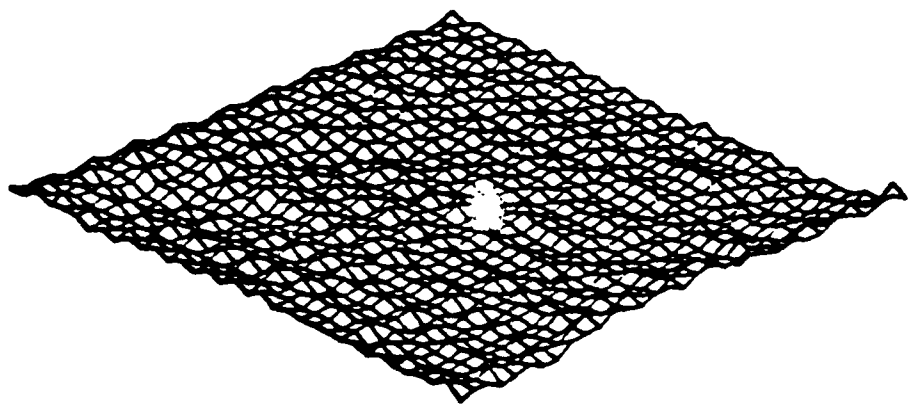

PEE 2 APR 80

HOT ALKALINE III - PREPARED 8:46, 2 APR 80
MAPPED 13:22, 2 APR 80

MIN =.2413E-01 NANO AMP
MAX =.5092E-01 NANO AMP
AVERAGE =.3508E-01 NANO AMP
STD DEVIATION =.1766E-01 NANO AMP

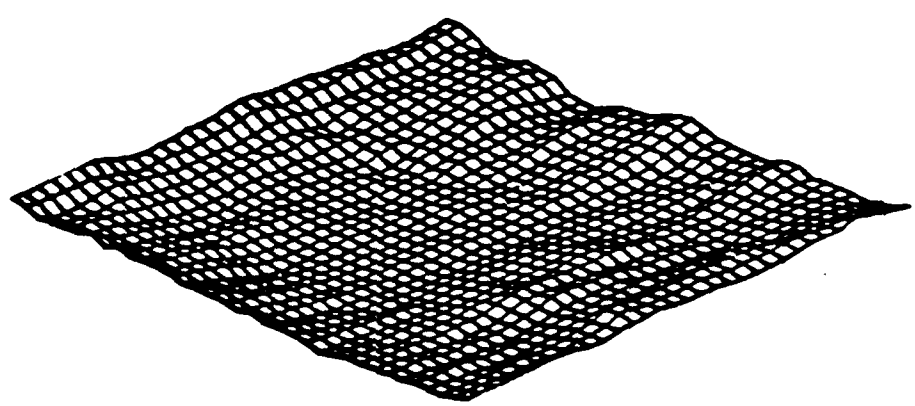

Fig. 12 PEE maps for sandblasted and alkaline cleaned samples.

the sandblasted surface. The larger PEE for the sandblasted surface may be associated with the thicker oxide layer. However, the attenuating properties of the outer contamination are not known at this point.

Each map demonstrates heterogeneity over the surface. More detailed studies will reveal the cause of the heterogeneity. The utility of these maps will be fully revealed when they can be compared with functional maps that indicate such things as corrosion resistance and coating adhesion strength or durability.

5. Phosphate Conversion Coatings

After pretreatment with some of the procedures of Table I, zinc phosphate coatings were applied and the deposition kinetics, the coating weight and the coating morphology determined. The phosphating solution was that used by Ghali and Potvin[8] and others (6.4 g/l ZnO, 14.9 g/l H_3PO_4, 4.1 g/l HNO_3 at 95°C). Potential-time curves were measured while the sample was immersed in the bath. After application of the coating, the samples were immediately neutralized in 0.3 w/o CrO_3 at 65 - 90°C for 3 min and aged at room temperature for at least 48h. For determination of the coating weight, the coating was stripped in 180 g/l NaOH + 90 g/l NaCN by repeated immersion until the weight of the sample did not change anymore.

a. Deposition Kinetics

As discussed by Ghali and Potvin[8] the change of the potential of steel in the course of phosphating is related to the nature of the compactness of the coating formed during the treatment. Gabe and Richardson[9,10] have attempted to correlated potential-time measurements with the physical properties of phosphate coatings.

Potential-time measurements have been performed for steel with different surface treatments in the zinc phosphate bath. The steel potential was measured vs SCE which was connected to the bath by a long Luggin capillary. A compensation circuit was used to accurately record the small potential changes during phosphating. Typical potential-time curves for four different treatments

are shown in Fig. 13 for a 30 min immersion period. The polished and degreased sample shows the largest potential change during phosphating (about 80 mV) similar to the schematic curves shown by Ghali and Potvin[8] for an electropolished mild steel. For the other treatments used here the potential change was about 40 mV or less, which is more in agreement with the results of Gabe and Richardson.[9,10] The potentials after 10 min and 30 min taken from two different series of measurements are shown in Table IV.

According to TT-C-490, the minimum coating weight for zinc phosphate is 300 mg/ft^2 or 0.32 mg/cm^2 for dip processes. The coating weights for the 13 different pretreatment procedures is also given in Table IV together with the weight loss of the steel surfaces during the coating formation. All coating weights are well in excess of the minimum weight of 0.32 mg/cm^2. The anodic etch, pickling in inhibited HCl, alkaline derusting, chemical smoothing and passivation in HNO_3 produced coatings which had ten times the minimum weight, while the thinnest coatings resulted after pretreatment by polishing and degreasing and by degreasing only. These surfaces also had by far the lowest metal loss. For all the other surface treatments the metal loss was between 1.18 and 1.49 mg/cm^2. Gabe and Richardson[10] reported a coating weight of 3.5 mg/cm^2 for mild steel pickled in 20 v/o HCl.

b. Morphology

The morphology of the zinc phosphate coatings formed on steel after the 13 different pretreatment procedures of Table IV was examined by SEM. Significant differences were noted for different pretreatments. The coating after degreasing only was fairly coarse consisting of a plate-like structure (Fig. 14a). Polishing (Fig. 14b) and sandblasting (Fig. 14c) produced a finer structure. The morphology of the coating after degreasing and the hot alkaline treatment was very similar. Pickling in inhibited HCl after degreasing and polishing produced the coarsest coating (Fig. 14d). The coatings produced by alkaline derusting, H_3PO_4, anodic etch, electropolishing (Fig. 14e) and chemical smoothing were all very similar.

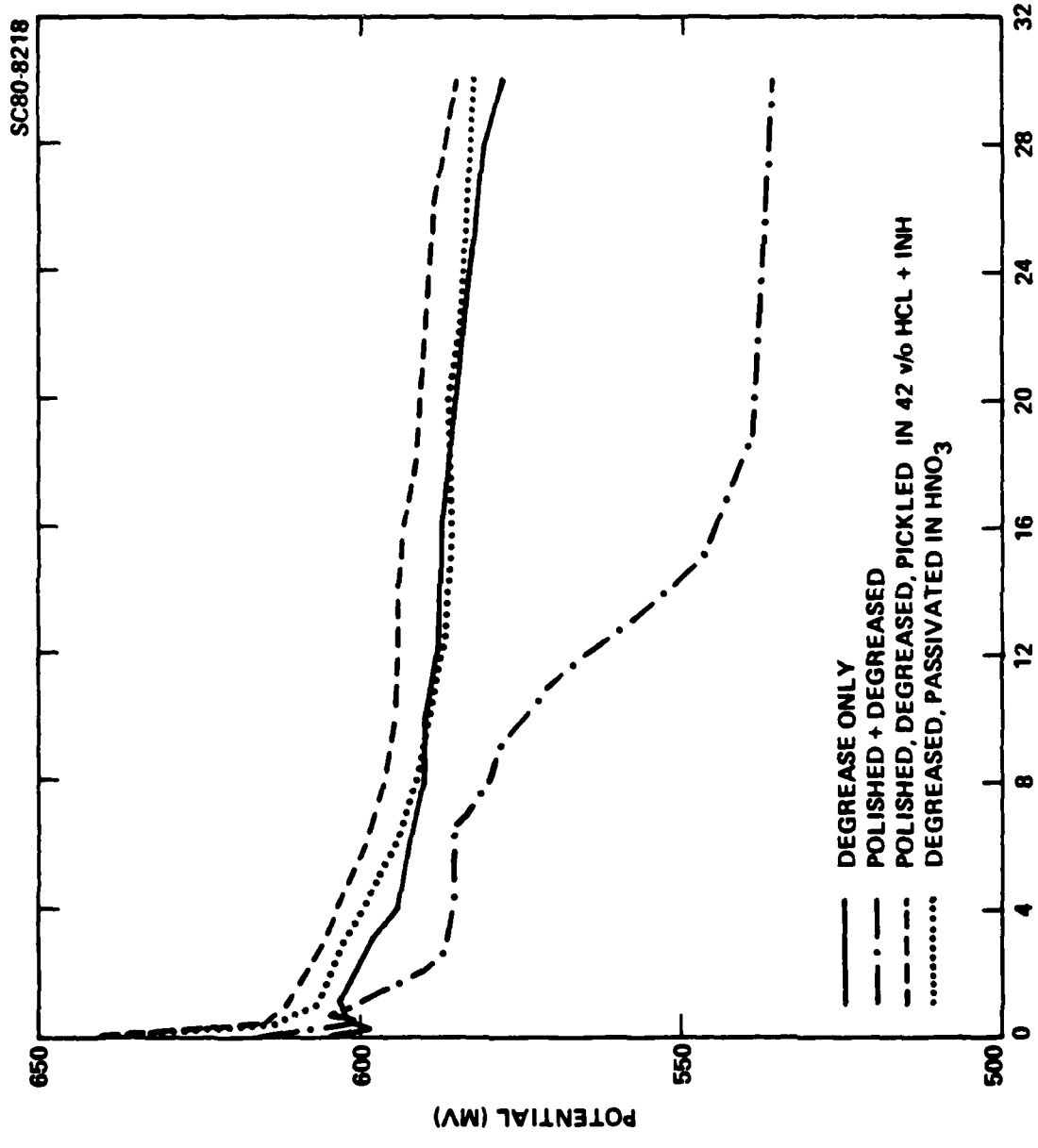

Fig. 13 Potential-time curves for steel of four different surface pretreatments immersed in phosphating solution.

Table IV

Coating Weight, Metal Loss and Potential for Zinc-Phosphating of 1010 Steel

Surface Treatment	Coating Weight (mg/cm^2)	Metal Loss (mg/cm^2)	$-E_{10}$ (mV)	$-E_{30}$ (mV)
Degrease (d)	1.78	0.74	579	578
Polish (p) & d	0.83	0.36	580	536
Sandblasted & d	3.04	1.18	-	591
d & Passivate in HNO_3	2.68	1.19	576	582
p & d & Passivate in HNO_3	3.40	1.27	593	-
d & 42 v/o HCl & Inhibitor	3.29	1.43	591	-
p & d & 42 v/o HCl & Inhibitor	4.30	1.39	584	585
d & hot alkaline	2.05	1.31	591	558
d & alkaline derusting	4.03	1.49	591	577
d & H_3PO_4 2.30	1.32	588	573	
d & anodic etch	4.41	1.42	588	584
d & electropolishing I	2.91	1.27	583	588
d & chemical smoothing	3.43	1.26	593	578

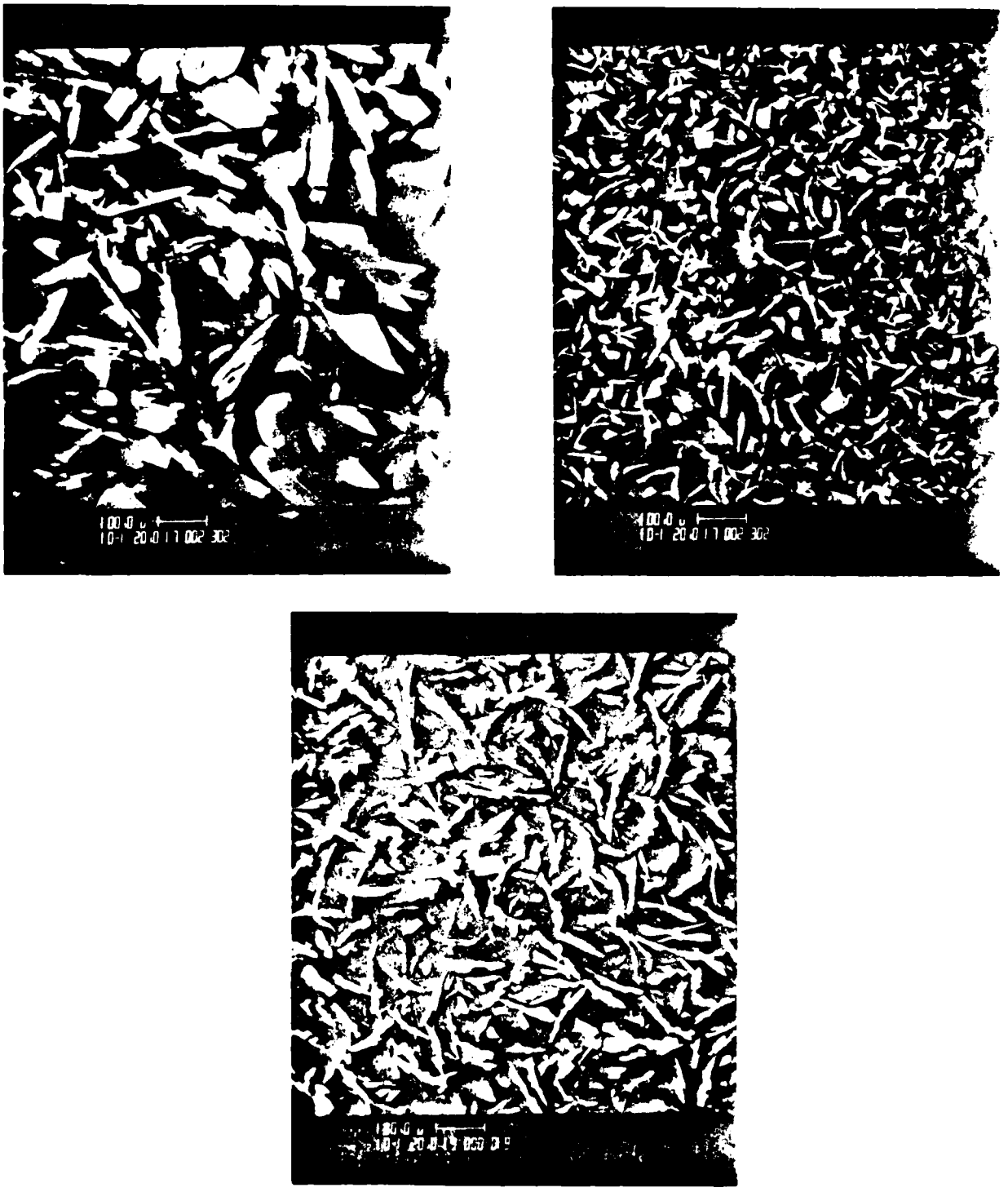

Fig. 14 Surface morphology of zinc phosphate conversion coating on steel for five different pretreatment procedures.

SC80-9091

Fig. 14 Continued.

Further testing of the properties of the iron phosphate coating formed on steel surfaces with different pretreatment procedures is necessary to understand the effects of surface structure on adhesion and corrosion protection of these coatings. Such tests are being intiated at present. At this time it is interesting to note that the polish-degrease pretreatment which showed the largest potential change (Fig. 13) produced the finest phosphate structure with the lowest coating weight, while additional pickling in inhibited HCl resulted in the coarsest surface structure with the second highest coating weight.

c. AC Impedance of Phosphated Steel

The shape of the electrochemical impedance vs frequency function for a surface at virtual open circuit can provide information on the corrosion kinetics[12] in a nondestructive manner. The frequency response reflects various forms of kinetic control of electrode processes, for example, by diffusion, charge transfer or adsorption.[16] In certain instances several electroactive adsorbed intermediates give discrete relaxations of the frequency response of the a.c. impedance.[17,18] Recently the a.c. impedance vs frequency behavior of polymer coated steel has lead to a model for the electrolytic degradation of polymer coated steel.[13-15] In recent years automated digital transfer function analyzers have made electrochemical impedance vs frequency data readily available to electrochemical researchers.[19]

The a.c. impedance of several phosphated steel specimens has been measured as a function of frequency. The resulting data provide some insights into the degree and mechanism by which phosphate coatings protect metal substrates. A summary of the experimental procedure, results and progress in the interpretation of these results follows.

Experimental Consideration

The Solarotron 1170 transfer function analyzer (TFA) provided the measurement of the correlation function, * of the phosphated

*$j^2 = -1$, ω = frequency in radians/second.

steel sample placed in a typically 0.6 M KNO_3, argon flushed, electrolyte. The sample was potentiostatically controlled at its corrosion potential using a PAR 173 potentiostat during the TFA measurement. The current output was taken from the Model 179 current amplifier. A 3.2 cm^2 1010 phosphated steel electrode served as the test specimen.

The measured transfer function is, of course, the complex, frequency dependent impedance, Z, which has both in-phase, Z_{in}, and out-of-phase components, Z_{out}. Alternatively, the data may be expressed as the impedance modulus, |Z|:

$$|Z| = \left(Z_{in}^2 + Z_{out}^2\right)^{1/2}$$

and phase:

$$\theta = \tan^{-1}\left(Z_{out}/Z_{in}\right) .$$

The specimens were degreased and electropolished (D+EP), degreased only (D), degreased and polished (D+P), degreased and polished and etched in inhibited HCl (DP/HCl+I), or degreased and etched in inhibited HCl (D/HCl+I) as described in Table IV.

Results of a.c. Impedance Measurement

Most of the phosphated steel specimens exhibit two relaxation times between 10^6 and 10^{-1} radians/second. For example, Fig. 15 shows the Bode plot of |Z| vs log ω, and θ vs log ω for a phosphated 1010 steel which was degreased and electropolished (D+EP) prior to the phosphate treatment. The presence of two broad peaks exhibiting maxima in θ appear for these systems and provide evidence for the two relaxation processes. In most observed instances the slowest process occurred at frequencies sufficiently low so that the low

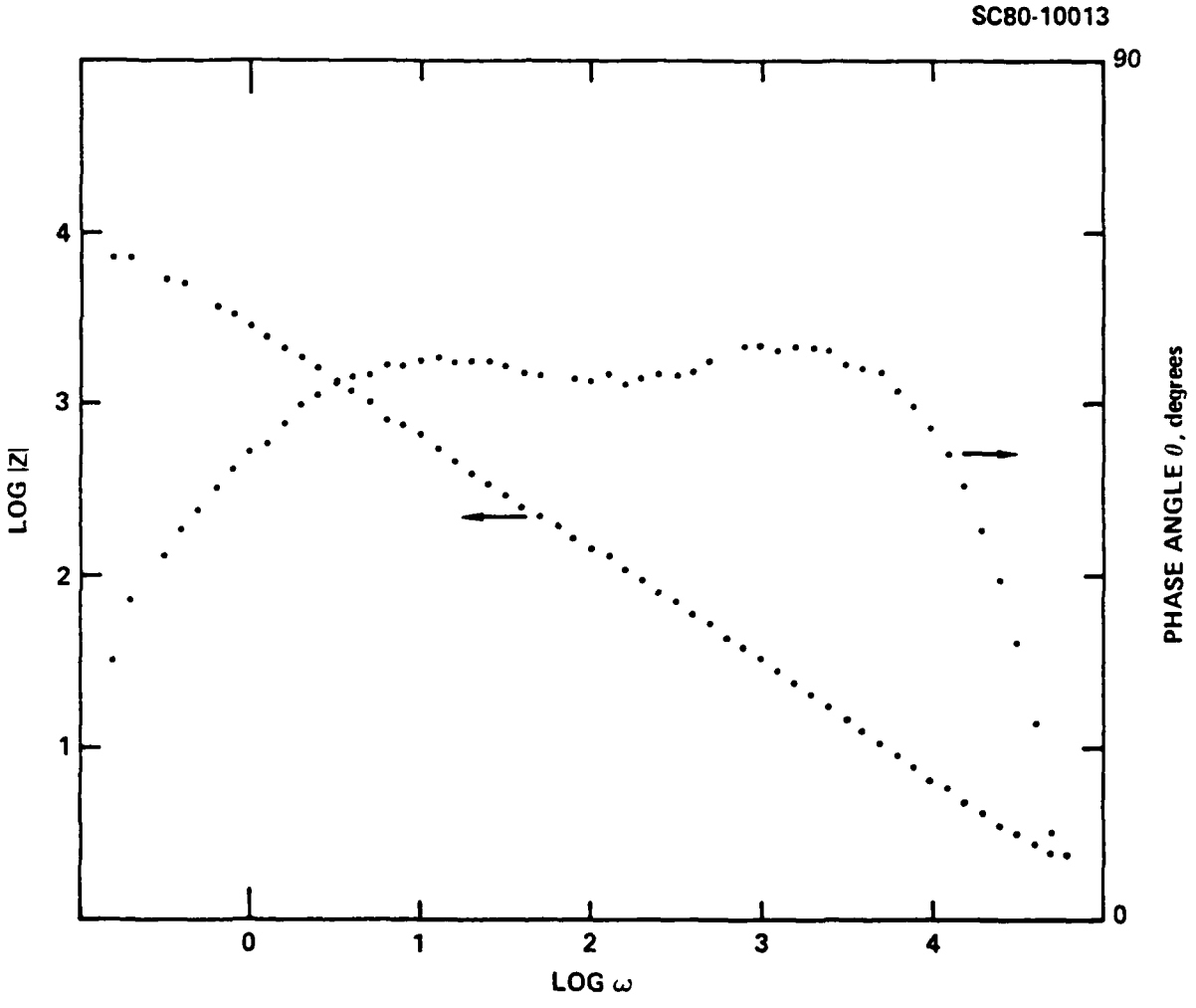

Fig. 15 Typical frequency dependence of |Z| and θ for a phosphated steel: D+EP after 22 hours in 0.6 M KNO_3.

frequency limit where |Z| becomes frequency independent, falls outside the range of the instrument. The frequencies of maximum θ define the respective high and low frequency characteristics.

Although either two maxima, or a maximum and a shoulder appear for the $\theta(\omega)$ function of phosphated steel samples placed in 0.6 M KNO_3, a decrease in the electrolytic resistance produced through the use of 0.06 M KNO_3 results in a θ spectrum having only one broad maximum, Fig. 16. This result is consistent with a parallel pore model, Fig. 17, which considers the electrochemical impedance as a parallel resistor/capacitor in series with a resistor representing electrolytic penetration of pores in the coating. Furthermore, the network which represents the pore is in parallel with a parallel resistor and capacitor representing the coating. A computer calculation for a model system shows that as the pore resistance increases, the two maxima in $\theta(\omega)$ coalesce to form one broad maximum, Fig. 18. Although the model must eventually be refined to include the distribution in relaxation times observed in practice, there does appear in these results qualitative confirmation of a porous penetration by the electrolyte of the phosphate coating.

The time variation of the high and low characteristic frequencies with time, which appear in Figs. 19 and 20 show an aspect which must also be considered before a quantitative model and mechanism of phosphate protection can be developed. The high frequency and low frequency characteristics appear to correlate negatively with each other, the characteristic frequencies for the respective maxima either diverge or converge with time as illustrated in Figs. 19 and 20. In no instance observed to date have both of these characteristic frequencies increased or decreased in a parallel fashion or has one changed without a change in the other. The divergent or convergent behavior is summarized in Table V.

This behavior cannot be predicted from independent variation of pore or coating impedances of the model since independent variation of pore or coating properties in the model will independently vary the maxima. For example, Fig. 21 shows a decrease in the frequency of the low frequency maximum only when

Table V
Summary of the Results of the Impedance of Phosphated Steel

Sample	Air Saturated	Behavior of Characteristic Frequencies	After 22 hrs θ_1 degrees	$\|Z_1\|$ ohms	θ_2 degrees	$\|Z_2\|$ ohms
D + EP	X	Diverge	60	13.7	46.5	4644
D + EP		Converge	60	29.0	60.0	457
D/HCl + I		Diverge	-	-	56.0	530
DP/HCl + I		Diverge	-	-	-	-
D	X	Diverge	47	22.0	43.0	2866
DAE		Converge	52	10.7	56.0	316
D + P		Diverge	36	16.5	59.0	823

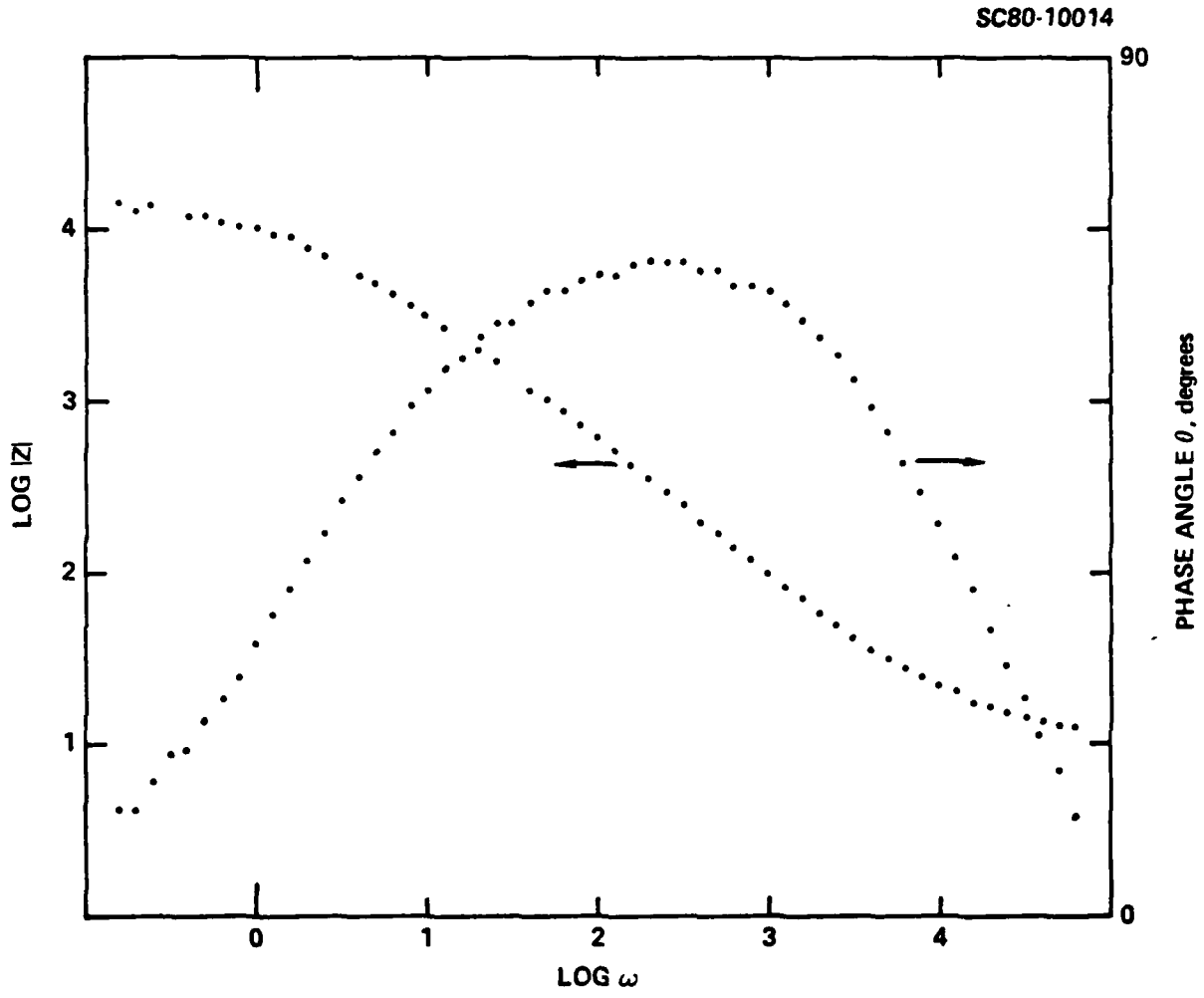

Fig. 16 Frequency dependence of |Z| and θ for a phosphated steel (D+EP) in 0.06 M KNO_3 after 22 hours.

SC80-9847

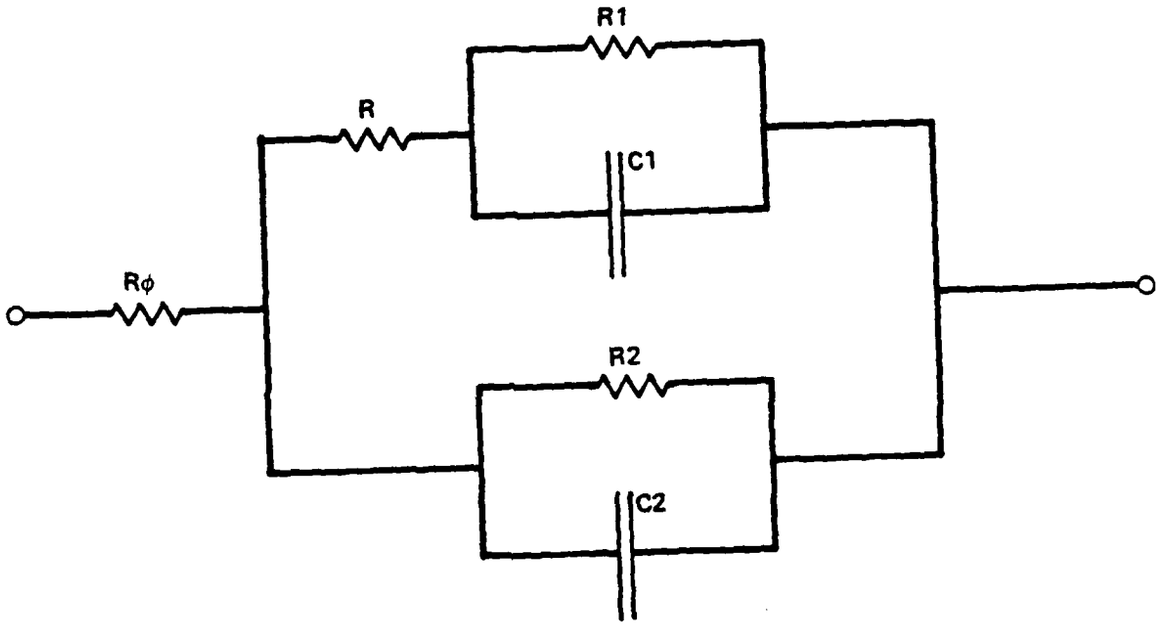

Fig. 17 Impedance analog for porous penetration model.

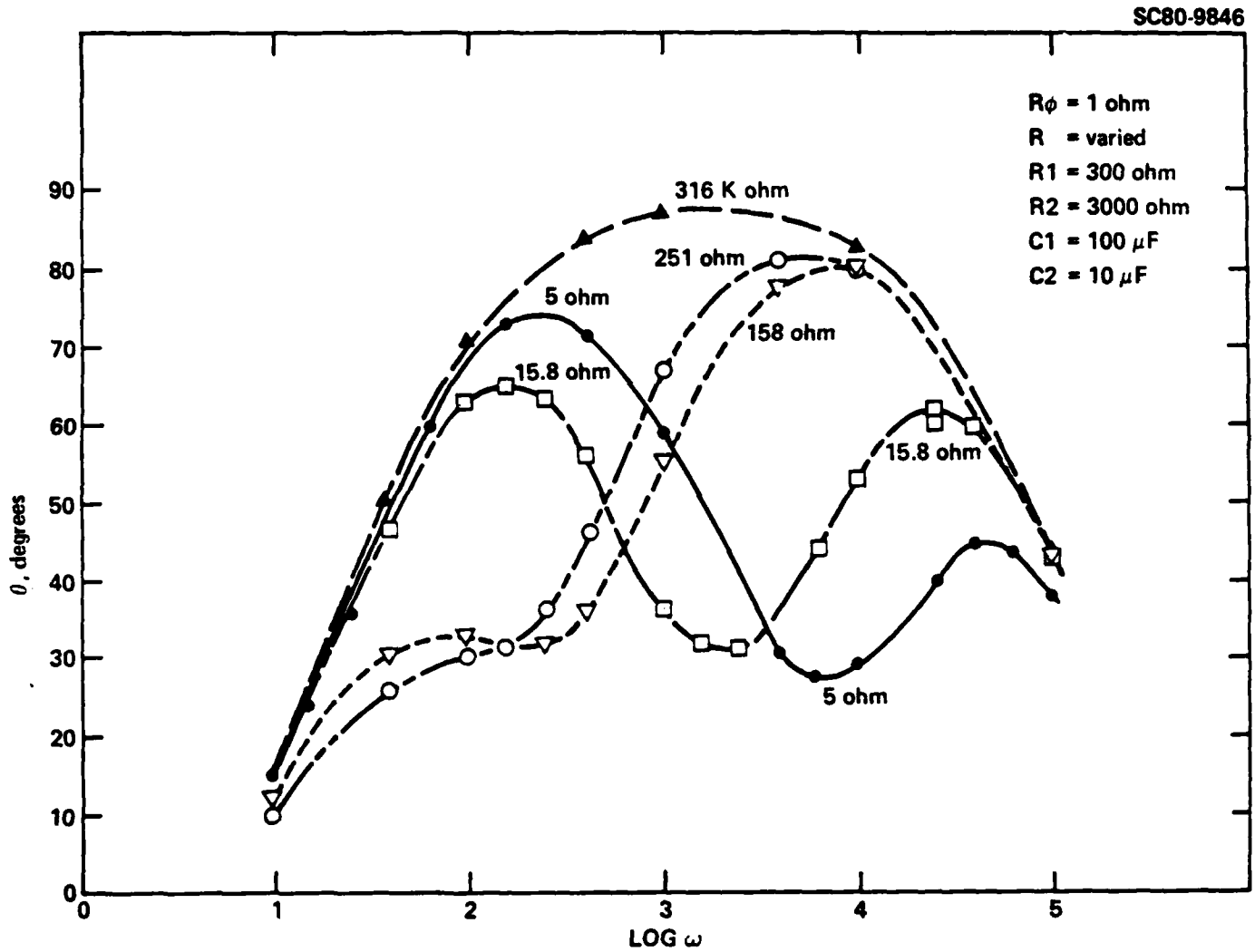

Fig. 18 Theoretical variation of θ spectrum with varied pore resistance.

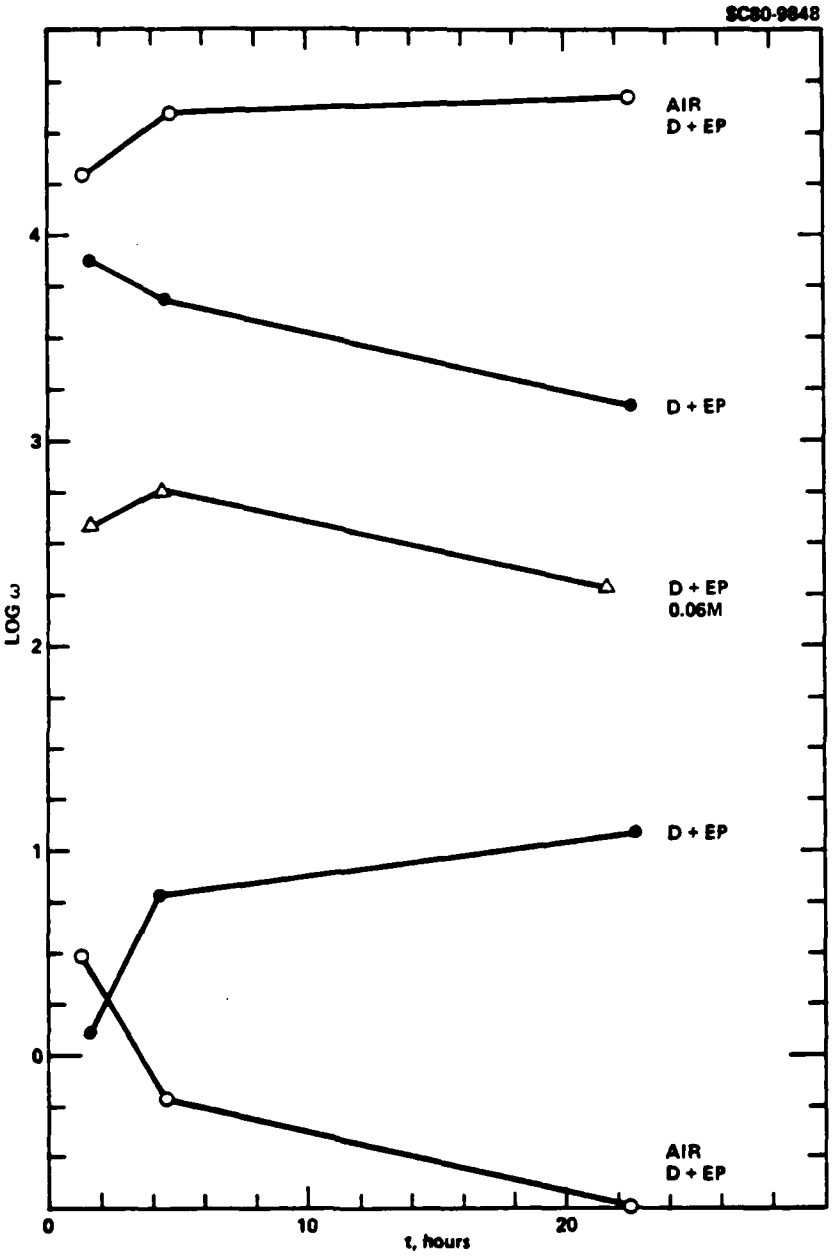

Fig. 19 Variation of the frequency characteristics, ω_1 and ω_2, with time for D+EP specimens.

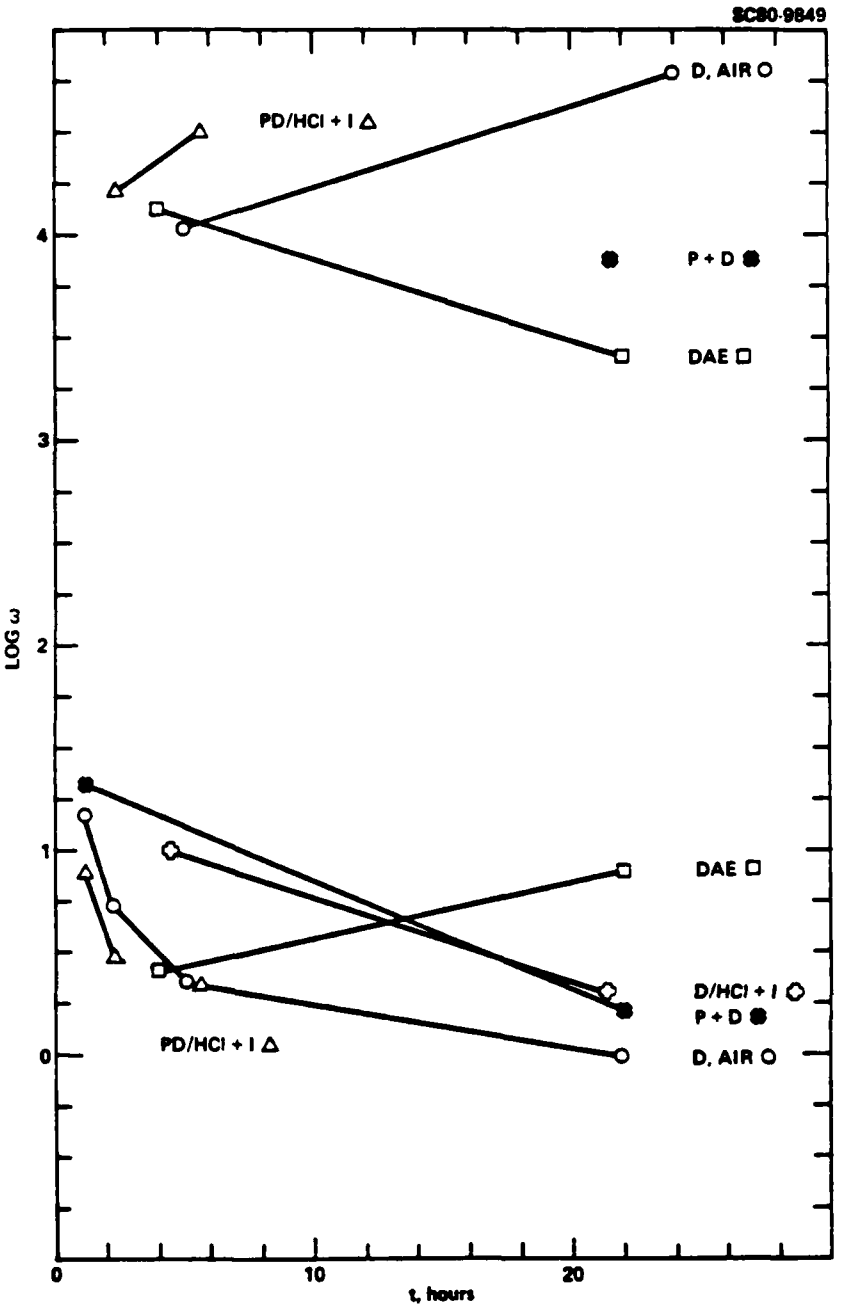

Fig. 20 Variation of the frequency characteristics, ω_1 and ω_2, with time for phosphated specimens.

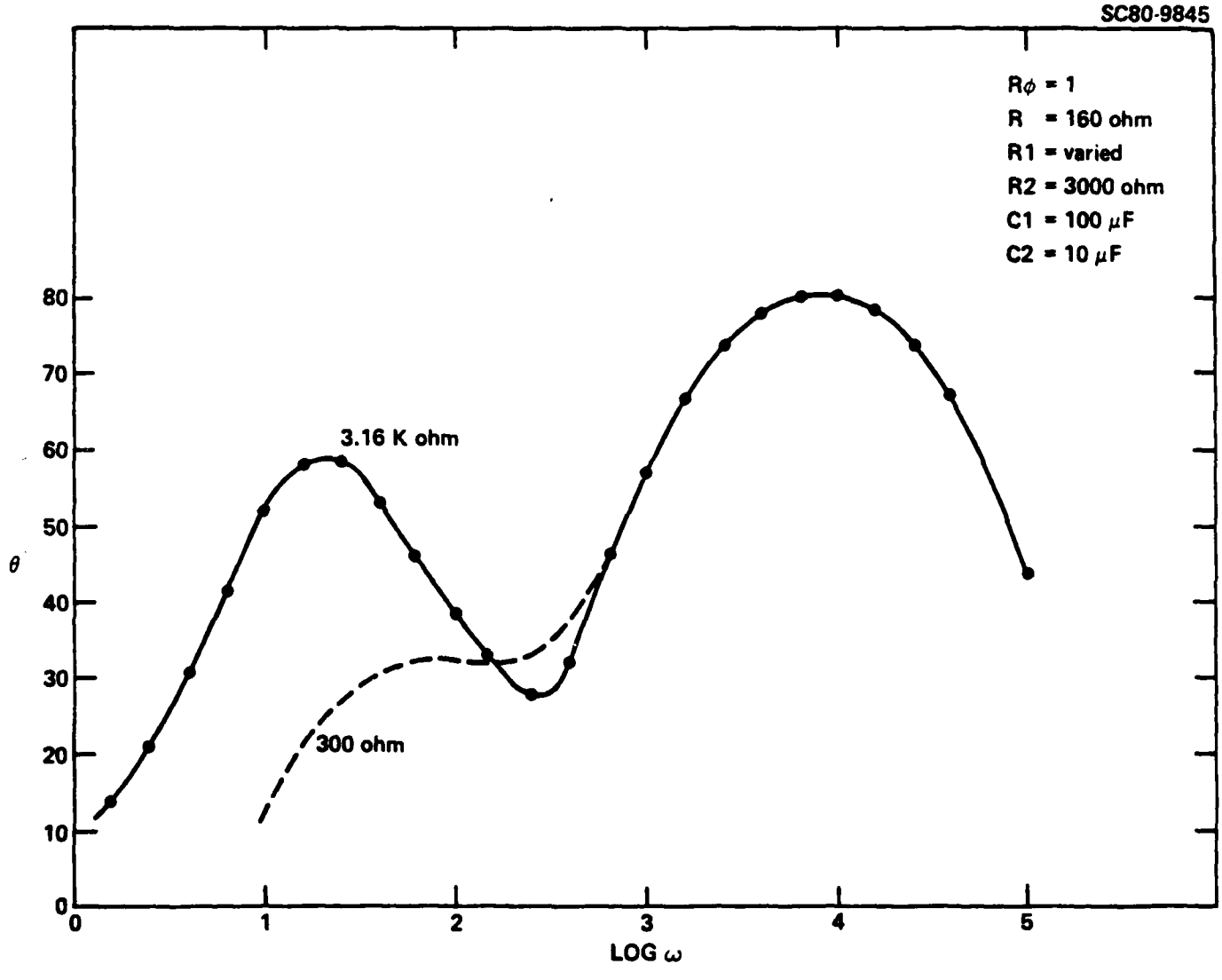

Fig. 21 Theoretical variation of θ behavior under independent variation of the pore element.

the resistor corresponding to the impedance at the bottom of the pore increases. However, this leaves the high frequency maximum unchanged.

The results show that the processes governing pore impedance and those governing coating impedance interact to produce the negative correlation in the time dependence of characteristic frequencies.

As a final point, the value of $|Z_2|$, at the absolute value of the impedance at the low frequency characteristic will provide the best correlation with d.c. polarization resistance. Actual extrapolation to R_p from $|Z_2|$ requires more specific mechanistic information not available at this time. Nevertheless, comparison of values of $|Z_2|$ in Table V is informative. The high values of $|Z_2|$ correlate with systems run under air saturation which could allow passivation of the interface at the bottom of the pores. The systems which show converging relaxation frequencies show the lowest $|Z_2|$ values.

More results will be obtained before a conclusion on the mechanism by which phosphate coatings protect carbon steel can be reached. However, evidence exists which suggests a porous coating in which electrochemical processes occurring across a coating interface are intimately coupled to the processes which occur at the pores. Chance and France[20] have invoked the coupling of phosphate coatings to electrochemical kinetics of metal dissolution through dissolved phosphate anions which would be consistent with these results.

IV. SUMMARY

The surface morphology, chemical composition of surface films and the activity of surface structures resulting from a number of different pretreatment procedures have been evaluated using scanning electron microscope (SEM), Auger electorn spectroscopy (AES, SAM), X-ray photoelectron spectroscopy (XPS), surface potential difference (SPD) and photoelectron emission (PEE) measurements. The deposition kinetics and surface morphology of zinc phosphate coatings have been determined. A.c.impedance measurements of phosphated steel have been determined as a function of time and frequency for several samples. The results show that surfaces to be polymer coated can have a variety of physical and chemical properties depending on the pretreatment and subsequent aging. These treatments can result in different kinetics of phosphate conversion coating and phosphate morphology. Results from a.c. impedance measurements of phosphated steel indicate a porous structure in which a complex coupling between the electrochemical properties of the coating and pores exists and oxygen produces an apparent beneficial effect on the corrosion behavior.

V. REFERENCES

1. S. Spring, "Preparation of Metals for Painting," Reinhold Publ. Corp., New York, 1965.

2. R.L. Snogren, "Handbook of Surface Preparation," Palmerton Publ. Co., New York, 1974.

3. J.A. Murphy (editor), "Surface Preparation and Finishes for Metals," McGraw-Hill Book Co., New York, 1971.

4. R.M. Burns and W.W. Bradley, "Protective Coatings for Metals," Reinhold Publ. Co., New York, 3rd Edition 1967.

5. D.H. Kaelble, Polymer Eng. and Sci. 17 (7), (1977).

6. D.H. Kaelble and P.J. Dynes, J. Colloid and Interface Sci. 52, 562 (1975).

7. T. Smith, J. Appl. Phys. 46, 1553 (1975).

8. E.L. Ghali and R.J.A. Potvin, Corros. Sci. 12, 583 (1972).

9. N. Helliwell, D.R. Gabe and M.O.W. Richardson, Trans. Inst. Metal Finish. 54, 185 (1976).

10. J.B. Lakeman, D.R. Gabe and M.O.W. Richardson, ibid. 55, 47 (1977).

11. J. Devay, F. Janaszik, L. Meszaros and F. Morkay, Acta Chim. Acad. Sci. Hung., Tomas 74, 199 (1972).

12. F. Mansfeld, "Recording and Analysis of AC Impedance Data for Corrosion Studies," submitted to Corrosion.

13. G. Reinhard, K. Hahn and B. Gorzolla, Plaste und Kautschuk 25, 548 (1978).

14. H. Potente and F. Stoll, Farbe und Lack, 81, 701 (1975).

15. H. Potente and E. Braches, Werkstoffe und Ihre Veredelung, 2, 13 (1980).

16. S. Haruyama, "Faradaic Impedance of Mixed Potential Electrode," Proc. 5th Int'l Conf. Met. Corr. (1972).

17. I. Epilboin and M. Keddam, J. Electrochem. Soc. 117, 1052 (1970).

18. R.D. Armstrong and M. Henderson, J. Electroanalytical Chem. 39, 81 (1972).

19. C. Gabrielli and M. Keddam, Electrochim. Acta, 19, 355 (1974).

20. R.L. Chance and W.D. France, Corrosion, 25(8), 329 (1969).

VI. APPENDIX:

SURFACE PREPARATION METHODS FOR FEDERAL SPECIFICATION TT-C-490B

Method I. Mechanical or abrasive cleaning. Samples were degreased according to Method II, below, and sandblasted with 10 μ aluminum oxide to white metal. After sandblasting the samples were degreased for a second time.

Method II. Solvent cleaning. Samples were degreased with trichloroethylene or 1, 1, 2, 2-tetrachloroethylene for 15 min in an apparatus providing both vapor and liquid cleaning.

Method III. Hot alkaline. Samples were immersed for 5 min in the solution composed of 75 g/l (10 oz/gal) of the mixture shown below, maintained at a rolling boil. The chemical composition of the mixture by weight and the solution concentration and temperature meet Federal Specification P-C-535B referenced in TT-490C.

Component	Weight % in Mixture	Concentration in Solution, g/l
Nacconol 90F[a]	23.7	17.8
Sodium metasilicate	31.3	23.4
Sodium dihydrogen phosphate	12.3	9.2
Trisodium phosphate	24.8	18.6
Triton X100[b]	7.9	5.9

a. Stepan Chemical Co., Northfield, Ill. A surfactant containing mainly sodium dodecylbenzene sulfonate.
b. Rohm and Haas Trademark Suppled by Eastman Kodak Company.

Method V. Alkaline derusting. The type II cleaning compound as described in MIL-C-14460B was used at 50°C with electrolytic action. A current density of 77 mA/cm^2 was reversed in polarity every minute ending with an anodic current. Afterward, samples were rinsed with water, then 0.5 v/o phosphoric acid. The cleaning compounds contained the following:

Component	Concentration, g/l
Sodium hydroxide	89
Sodium cyanide	74
Disodium ethylenedinitrilo tetraacetate (EDTA)	74

Method VI. Phosphoric acid Samples were immersed at 80°C for 5 min in the solution:

Component	Concentration
Phosphoric acid	8.5 v/o
Diethylthiourea[a]	0.5 g/l
Nacconol 90F[b]	1.8 g/l

a. An inhibitor

b. See Method III.

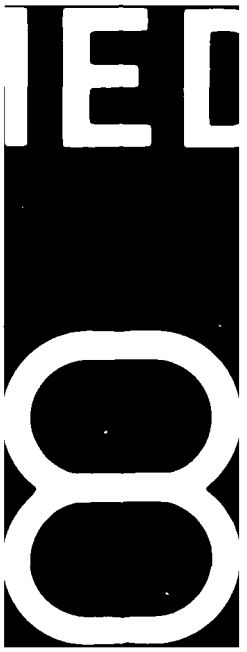
IED
8